People's Democratic Republic of Algeria

Ministry of Higher Education and Scientific Research

UNIVERSITY CHADLI BENDJEDID - EL TARF جامعة الشاذلي بن جديد-الطارف

FACULTY OF SCIENCE AND TECHNOLOGY
PHYSICS DEPARTMENT

MASTER MEMORY

DOMAIN: MATTER SCIENCE

SECTOR: Physics

OPTION: Physics of Materials

Theme

Analysis of physical properties of chalcogenides CaSe and ZnSe using FP-LAPW method

Presented by :
DJEBALI Djihen

Directed by :
GUENFOUD Fatma

Members of the Jury

Dr. TOUAM Selma	President	MCA	El Tarf University
Dr. GUENFOUD Fatma	Supervisor	MCB	El Tarf University
M^{s} GASMALLAH Amel	Co-supervisor	DOCT	El Tarf University
Dr. BOUZIDA Amel	Examiner	MCB	El Tarf University

University Year : 2024/2025

Thanks

Praise be to God, first and last, outwardly and inwardly, by whose grace good deeds are completed, and by His alone guidance, I was able to reach this stage of my academic journey.

I extend my heartfelt gratitude and profound appreciation to my esteemed supervisor, Dr.Guenfoud Fatma who has been an excellent companion and supporter with her knowledge, patience, and continuous encouragement. Her guiding touches were instrumental in overcoming many challenges, and her contributions had a significant impact on this work.

I would also like to extend my gratitude to Dr. who accom Touam Selma panied me with her appreciation and care, and whose words always brought me reassurance and confidence, and to . Ms Gasmallah Amel, who generously gave me her time and attention, leaving positive remarks that I cherish.

And I must express my gratitude to Dr. Bouzida Amel for her honor and kind attention to this work.

And finally, I extend heartfelt thanks to Ms Gacem Marwa, who has been a sincere support during moments of fatigue, and whose gentle hand was present when I needed assistance.

To all of you, heartfelt thanks and prayers, and I ask God to reward you all abundantly on my behalf.

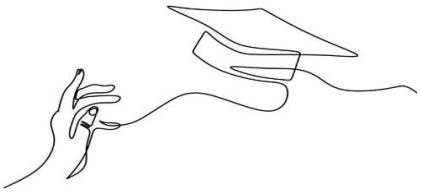

Dedications

By the care of Allah and all the courage and patience He has given me over these years of study, I am now able to see the fruit of my labor in this modest dissertation.

I dedicate this work.

To my father, who taught me that ambition has no limits, and whose prayers were my strength at every moment.

To my mother, the source of tenderness, who were my motivation and drive, the hand that wiped away my exhaustion, and the smile that brought me back tolife.

To my brother Farouk, my support and friend, whose strength I leaned on whenever I stumbled.

To my brother Ziad, who was always by my side, with his smile and words that lightened my burdens.

To my fiancé, my future life partner — thank you for believing in me and sharing this dream and prayer.

To my dear friend Nardjes, who stood by me through hard days and beautiful moments — your presence was a blessing beyond words.

And to my entire family, who have always been my warm and loving haven…

Especially Inas and Roumayssa, I say: you are the most beautiful part of this journey, and my gratitude to you cannot be put into words.

This success is not mine alone… it belongs to all of you.

Abstract

In this work, we studied the structural, electronic and Optical properties of binary compounds CaSe and ZnSe by the augmented and linearized plane wave method ***(FP-LAPW)***, based on the density functional theory ***(DFT)*** implemented in the ***Wien2K*** code. We have used the generalized gradient approximation ***(GGA)*** for the term of the potential for exchange and correlation ***(XC)*** to study the structural properties.

The calculation of the structure of electronic bands was carried out in the approximation generalized gradient ***(WC-GGA)*** and ***mBJ***.

The study of the electronic structure of the binary compounds CaSe and ZnSe has been carried through the calculation of the band structure, total and partial electronic density of states diagrams ***(TDOS*** and ***PDOS).***

We have also analyzed the optical properties (dielectric function, refractive index, the absorption coefficient, the reflection coefficient and the energy loss coefficient).

Several calculated results have been compared with available experimental and other theoretical data.

Keywords: FP-LAPW, DFT, Binary compounds, GGA, mBJ.

Résumé

Dans ce travail, nous avons étudié les propriétés structurelles, électroniques et optiques des composés binaires CaSe et ZnSe par la méthode des ondes planes augmentées et linéarisées (FP-LAPW), basée sur la théorie de la fonctionnelle de densité (DFT) implémentée dans le code Wien2K. Nous avons utilisé l'approximation du gradient généralisé (GGA) pour le terme du potentiel d'échange et de corrélation (XC) afin d'étudier les propriétés structurelles.

Le calcul de la structure des bandes électroniques a été réalisé dans l'approximation du gradient généralisé (WC-GGA) et mBJ.

L'étude de la structure électronique des composés binaires CaSe et ZnSe a été réalisée par le calcul de la structure de bande, des diagrammes de densité d'états électroniques totale et partielle (TDOS et PDOS).

Nous avons également analysé les propriétés optiques (fonction diélectrique, indice de réfraction, coefficient d'absorption, coefficient de réflexion et coefficient de perte d'énergie).

Plusieurs résultats calculés ont été comparés aux données expérimentales et théoriques disponibles.

Mots-clés : FP-LAPW, DFT, Composés binaires, GGA, mBJ.

ملخص

في هذا العمل، قمنا بدراسة الخصائص البنيوية والإلكترونية والبصرية للمركبات الثنائية CaSeو ZnSe باستخدام طريقة الموجة المستوية المعززة الخطية (FP-LAPW) ، استنادًا إلى نظرية الكثافة الوظيفية (DFT) المطبقة في كود Wien2K.

استخدمنا تقريب التدرج المعمم (GGA) لمصطلح جهد التبادل والارتباط (XC) لدراسة الخصائص البنيوية.

تم حساب بنية النطاق الإلكتروني باستخدام تقريب التدرج المعمم (WC-GGA) و mBJ.

تمت دراسة البنية الإلكترونية للمركبات الثنائية CaSe و ZnSe من خلال حساب بنية النطاق، ومخططات الكثافة الإلكترونية الكلية والجزئية للحالات (TDOS و.PDOS) .

كما قمنا بتحليل الخصائص البصرية (الدالة العازلة، ومعامل الانكسار، ومعامل الامتصاص، ومعامل الانعكاس، ومعامل فقدان الطاقة).

قورنت العديد من النتائج المحسوبة بالبيانات التجريبية والنظرية المتاحة.

الكلمات المفتاحية : FP-LAPW ، DFT، مركبات ثنائية، GGA، mBJ

Contents

Thanks i
Summary ii
Abstract iii
Résumé iv
ملخص v
Table of Contents vi
List of figures ix
List of tables x
Abbreviations xi
INTRODUCTION GENERALE 02

Chapter I Presentation and originalities of the materials studied

I.1. Introduction 06

I.2. Semiconductor 06

I.2.1. Definition of II-VI Semiconductors 06

I.2.2. The different Types of Semiconductors 07

I.2.2.1. Extrinsic Semiconductors 07

I.2.2.2. Extrinsic Semiconductors 07

I.3. Direct and Indirect Bandgaps 08

I.4. Physical Properties 09

I.4.1. Characteristic of each element 09

I.4.2. Electronic Configuration of Compounds 10

I.4.3. Crystallographic Structure of the Binary Compounds CaSe and ZnSe 10

I.4.3.1. Description of the rock-salt NaCl structure (CaSe) 10

I.4.3.2. Description of the Zinc Blende structure (ZnSe) 11

I. 5. First Brillouin zone 12

I. 5. 1. Points of high symmetry 12

I. 5. 2. Lines of high symmetry 13

I. 6. Previous work on the study compounds 14

I. 6.1. Compound CaSe 14

I. 6.2. Compound ZnSe 15

References 16_17

CHAPTER II: Theoretical notions and calculation methods

II.1. Introduction 19

II.2. Schrödinger Equation 19

II.3. Fundamental Approximations 20

II.3.1. Born-Oppenheimer Approximation 20

II.3.2. The Hartree and Hartree-Fock Approximation 20

II.3.3. Density Functional Theory (DFT) 22

II.3.3.1. Problem Statement 22

II.3.3.2. Hohenberg-Kohn Theorems 22

II.3.3.3. Kohn and Sham Approach 23

II.3.3.4. The exchange-correlation functional 25

a- Local Density Approximation (LDA) 23

b- Approximation of the generalized gradient GGA 24

c- mBJ Potential 24

II.3.3.5. Solution of the Kohn-Sham Equations 27

II.4. Augmented and Linearized Plane Wave Method (FP-LAPW) 28

II.5. THE WIEN2K CODE 29

II .5.1 Wien2K Algorithm 30

II .5.2. The SCF calculation 31

II .5.3. Calculation of properties 32

References 33_34

CHAPTER III : Results and discussions

III.1. Introduction 36

III.2. Calculation details 36

III.3. Results and discussion 37

III.3.1. Structural properties of CaSe and ZnSe compounds 37

III.3.2. Electronic properties 39

III.3.2.a. Band structure and energy gap 39

III.3.2.b. Density of states 41

III.3.3. Optical properties 44

III-3-3.1. Results and discussions 46

a. Imaginary part of the dielectric function 46

b. Real part of the dielectric function 46

c. Refractive index 47

d. The reflectivity 48

e. Absorption 49

f. Electron energy loss spectrum 50

References 51_52

List of Figures

Figure	Title	*Page*
	Chapter I	
Figure I.1	*N-type Semiconductor*	**8**
Figure I.2	*P-type Semiconductor*	**8**
Figure I.3	*Energy band structure of (a) direct bandgap and (b) indirect bandgap*	**9**
Figure I.4	*NaCl crystal structure*	**11**
Figure I.5	*Crystal lattice of the Zinc-blende structure.*	**12**
Figure I.6	*First Brillouin Zone (zinc-blende, NaCl) with the representation of points and lines of high symmetries*	**13**
	Chapter II	
Figure.II.1	*Interdependence of the Kohn-Sham equations*	**25**
Figure.II.2	*Diagram of the self-consistent calculation of Density Functional Theory*	**28**
Figure.II.3	*Distribution of atomic unit cells adopted in the APW method: muffin-tin* spheres (S) of radius R_{MT} and interstitial region (1).	**30**
Figure.II.4.	*Wien2k code*	**32**
	ChapterIII	
Figure.III-1	*Variation of total energy as a function of volume of binary compounds CaSe and ZnSe in zinc blende and NaCl structures calculated by (WC-GGA).*	**38**
Figure.III-2	*Band structure of CaSe and ZnSe compounds using mBJ approximation*	**40**
Figure.III-3	*Total and partial density of states (DOS) of CaSe and ZnSe compounds using the mBJ approximation.*	**43**
Figure.III-4	*Variation of the imaginary part of the dielectric function as a function of energy for binary compounds CaSe and ZnSe*	**46**

Figure.III-5	*Variation of the real part of the dielectric function as a function of energy for the binary compounds CaSe and ZnSe.*	**47**
Figure.III.6.	*Variation of the refractive index as a function of energy for the binary compounds CaSe and ZnSe*	**47**
Figure.III.7.	*Variation of reflectivity as a function of energy for binary compounds CaSe and ZnSe*	**49**
Figure.III.8.	*Variation of absorption coefficient as a function of energy for CaSe and ZnSe binary compounds.*	**50**
Figure.III.9.	*Variation of the energy loss coefficient as a function of energy for the binary compounds CaSe and ZnSe.*	**50**

List of Tables

Tableau	***Title***	***Page***
	Chapter I	
TableI.1	*Characteristics of Ca, Se and Zn*	**10**
Table I.2	*Selected Portions of Mendeleev's Periodic Table*	**10**
TableI.3	*Atomic number and electronic configuration of the elements studied.*	**10**
	Chapter III	
Table III.1	*Lattice parameter a in (Å),bulk modulus B in (GPa) for the binary compounds CaSe and ZnSe compared to other experimental and theoretical data.*	**38**

Table III.2	*Energy gaps of the compounds CaSe and ZnSe (in eV) with the different approximations (WC-GGA), and mBJ compared to other experimental and theoretical results*	**41**
Table III .3	*Static dielectric function $\varepsilon_1(0)$ and static refractive index n(0) calculated for binary compounds CaSe and ZnSe.*	**48**

List of abbreviations

Symbol	Abbreviations
Ca	Calcium
Zn	Zinc
Se	Selenium
CaSe	Calcium Selenide
ZnSe	Zinc Selenide
ZB	Structure Zinc-blende
Cfc	Face-centered cubic
Ef	fermi energy
Ev	Valence energy
Ec	Conduction energy
BV	Valence band
BC	Conduction band
C°	Degree Celsius
cm3	Cubic centimeter
Pa	Pascal
eV	Electron-volt
A°	Angstrom
GHz	Giga-Hertz
Gpa	Giga-Pascal
PDOS	Partial density of states
TDOS	Total density of states
DFT	Density functional theory.
LDA	Local density approximation
GGA	Generalized Gradient Approximation
FP LAPW	Augmented and linearized plane wave method
WC-GGA	Generalized Gradient Approximation parameterized by **Wu and Cohen**

Introduction Générale

General Introduction

Materials science plays a very important role in technological developments, and this role continues to grow in many fields. In the field of solid-state physics, semiconductors are among the most widely used materials in advanced technologies and are the most extensively studied, especially binary semiconductors. These compounds have been often worn in domains of materiality and band structure countenances and have a range of desirable properties that can be exploited in electronic sensors and circuits **[1], [2], [3], [4], [5]**. II-VI semiconductor compounds are those materials formed of a metal from either group 2 or 12 of the periodical table (the alkaline earth metals and group 12 elements, in the past appealed groups II A and II B) and a nonmetal from group 16 (the chalcogens, in the past appealed group VI). Recently, group-II-VI semiconductors have brought a lot of care. This is owing to their aspiring employment in electronics and optoelectronic devices which vary from blue to near-ultraviolet spectral area **[6], [7]**. They have many implementations scoping from catalysis to microelectronics. These materiality are commonly differentiated by their band-gaps. They crystallize in the zinc-blende, the wurtzite or the rock-salt (NaCl) structures **[8], [9], [10]**.

Studying the physical properties of these compounds requires accurate theoretical models, due to the difficulty and cost of experimental work, especially at unusual temperatures and pressures. One of the most accurate theoretical methods for calculating electronic structure and crystalline properties is the FP-LAPW (Full-Potential Linearized Augmented Plane Wave) method. This method is based on density functional theory (DFT) and is known for its high ability to realistically and accurately describe the behavior of electrons in solids.

The aim of this thesis is to study the structural, electronic, and optical properties of the binary compounds CaSe and ZnSe, using the Wien2K simulation code with the linearized augmented plane wave (FP-LAPW) method within the framework of DFT density functional theory.
Following this introduction, the thesis is organized around three chapters:
The first chapter presents a detailed literature review, in which we present the materials used and describe their general physical properties.

The second chapter is devoted to a review of DFT density functional theory, the approximations used to treat the exchange and correlation potential, the principle of the FP-LAPW method, and the algorithm of the Wien2K computer code.

The third chapter summarizes the results obtained during our study, their interpretations, and a comparison with some available theoretical and experimental work.

Finally, our manuscript concludes with a general conclusion summarizing the essence of our results.

References

[1] Bhattacharya P., Fornari R., Kamimura H. (Eds.), Comprehensive Semiconductor Science and Technology, Elsevier Science (2011)

[2] Olloway P.H., McGuire G.E. (Eds.), Handbook of Compound Semiconductors: Growth, Processing, Characterization and Devices (1996)

[3]Buschow K.H.J., Flemings M.C., Kramer E.J., Veyssière P., Cahn R.W., IIschner B., Maha jan S. (Eds.), Encyclopedia of Materials: Science and Technology (2001)

[4] T. Yue, Y. Sun, Y. Zhao, S. Meng, Z. Dai Thermoelectric performance in the binary semiconductor compound A_2Se_2(A = K, Rb) with host-guest structure Phys. Rev. B, 105 (2022), Article 054305

[5] I. Vurgaftman, M.P. Lumb, J.R. Meyer Basics of crystal structure and band structure Chap., 1 (2020),

[6] T.-T. Fang Elements of Structures and Defects of Crystalline Materials Elsevier (2018)

[7] M. Afzaal, P. O'Brien Recent developments in II-VI and III-VI semiconductors and their applications in solar cells J. Mater. Chem., 16 (2006), pp. 1597-1602

[8] N. Mishra, G. Makov A novel interstitial site in binary rock-salt compounds Materials (Basel), 15 (2022), p. 6015

[9] J.E. Jaffe, R. Pandey, A.B. Kunz Electronic structure of the rocksalt-structure semiconductors ZnO and CdO Phys. Rev. B, 43 (1991), pp. 14030-14034

[10] A. Bouarissa, A. Gueddim, N. Bouarissa, S. Djellali Band structure and optical properties of polyaniline polymer material Polym. Bull., 75 (2018), pp. 3023-3033

Chapter I

Presentation and originalities of the materials studied

I.1. Introduction

Class II-VI semiconductors have attracted considerable interest from both experimental and theoretical points of view **[1]**, due to their potential technological applications ranging from the blue spectral region to the near ultraviolet region **[2]**. They are characterized by a wide band gap **[3]**, and most of them, particularly those of group IIAVIA, crystallize in the Rocksalt (NaCl) structure **[4]** and those of group IIB-VIA crystallize in the Zinc blende structure under normal conditions **[5]**. This type of semiconductor has bonds that become increasingly ionic due to the transfer of electronic charge from the group II atom to the group VI atom **[6]**. This favors their use in optoelectronic devices and in thin films **[7]**. These compounds are also of remarkable interest given the simplicity of their synthesis and the good optical results obtained **[8]**.

This first chapter provides a bibliographic review of the general physical properties of the binary compounds CaSe and ZnSe. It includes a description of the rocksalt and zinc blende crystal structures, followed by an overview of previous theoretical and experimental studies conducted on these materials.

I.2. Semiconductor

I.2.1. Definition of II-VI Semiconductors

A II-VI semiconductor is a compound material formed by combining one or more elements from group II of the periodic table (such as calcium, zinc, cadmium) with one or more elements from group VI (such as oxygen, sulfur, selenium, tellurium).

These materials are widely studied due to their desirable properties:

- High chemical and mechanical stability
- Good thermal conductivity
- Wide bandgap energies
- Direct bandgap nature, which makes them suitable for optoelectronic applications

A compound exhibits semiconducting behavior when the total number of valence electrons from its constituent elements equals eight.

In this context, calcium selenide (CaSe) and zinc selenide (ZnSe) are binary II-VI semiconductors formed by combining a group II element—calcium (Ca) or zinc (Zn)—with selenium (Se), a group VI element.

This work focuses on these binary compounds, CaSe and ZnSe, due to their potential applications in optoelectronics, including LEDs, laser diodes, and photovoltaic devices.

I.2.2.The different Types of Semiconductors

I.2.2.1. Intrinsic Semiconductors

An intrinsic semiconductor is a pure material in which the number of free electrons is equal to the number of holes. The concentration of impurities is extremely low—less than one impurity atom per 10^{13} host atoms.

I.2.2.2. Extrinsic Semiconductors

An extrinsic semiconductor is an intrinsic material that has been intentionally doped with specific impurities to modify its electrical properties, making it suitable for use in electronic components (such as transistors and diodes) and optoelectronic devices (like light emitters and detectors).

There are two main types of doping:

N-type Semiconductor

N-type dopants, also called donors, are elements or compounds with five or more valence electrons. When introduced into the intrinsic material, four of their electrons form covalent bonds with neighboring atoms, while the fifth electron becomes free to conduct electricity. In N-type semiconductors, electrons are the majority charge carriers, while holes are the minority carriers.

P-type Semiconductor

P-type dopants, known as acceptors, have three valence electrons. When incorporated into the semiconductor, they create "holes" by accepting electrons from neighboring atoms. In P-type semiconductors, holes are the majority charge carriers, and electrons are the minority carriers

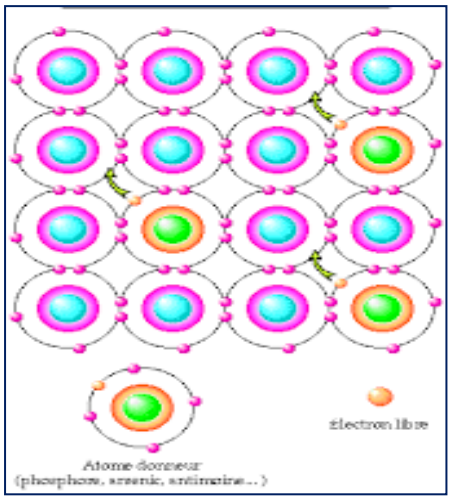

Figure I.1. *N-type Semiconductor*

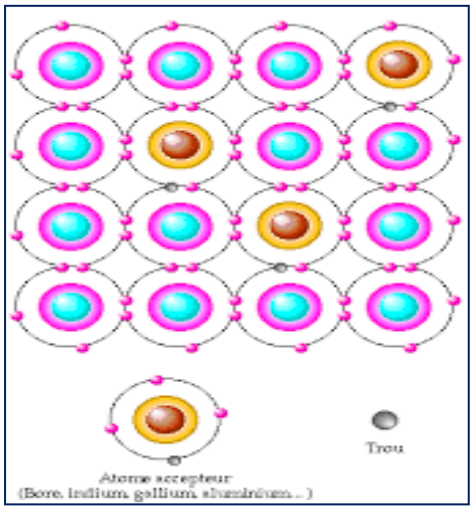

Figure I.2. *P-type Semiconductor*

I.3. Direct and Indirect Bandgaps

The energy band diagrams illustrated in Figure (I.3) highlight two fundamental types of semiconductors:

direct bandgap semiconductors, the conduction band minimum and the valence band maximum occur at the same wave vector $\vec{k}$, typically at the center of the Brillouin zone ($\vec{k}$ = **0**). This alignment allows electronic transitions to occur without a change in momentum.

indirect bandgap semiconductors have their valence band maximum and conduction band minimum located at different wave vectors $\vec{k}$. As a result, momentum is not conserved during electron transitions between these bands.

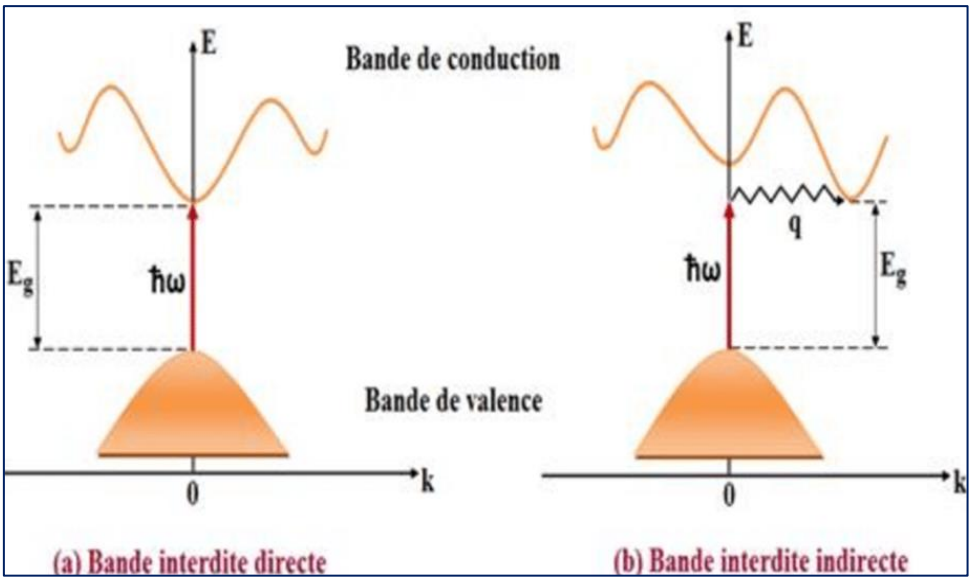

***Figure I.3**. Energy band structure of (a) direct bandgap and (b) indirect bandgap*

I.4. Physical Properties

I.4.1. Characteristic of each element

Here is a table presenting some fundamental data about the elements Ca, Se and Zn:

Element	Ca	Se	Zn
Designation	**Calcium**	**Selenium**	**Zinc**
Atomic number	**20**	**34**	**30**
Year of discovery	**1808**	**1817**	**1746**
Land of discovery	**UK**	**Sweden**	**Germany**
Classification	**Alkaline earth metal**	**Non-metals**	**Transition metal**
Band	**IIA-B**	**VIA**	**IIA-B**
Period	**4**	**4**	**4**
Relative atomic mass	**40.08 u**	**78.96u**	**65.38 u**
Melting temperature	**842 °C**	**221 °C**	**419.5 °C**
Density	**1.55 g/cm³**	**4.81 g/cm³**	**7.14 g/cm³**
Types of crystal lattice structure	**Face-Centered Cubic (FCC)**	**Hexagonal**	**Hexagonal**

***Table I.1** .Characteristics of Ca, Se and Zn*

I.4.2. Electronic Configuration of Compounds

The classification of the constituent elements of our CaSe and ZnSe compounds is shown in Table (I.2)

IA-B	IIA-B	III_A	IVA	VA	**VIA**	VIIA
Li^3	Be^4	B^5	C^6	N^7	O^8	F^9
Na^{11}	Mg^{12}	Al^{13}	Si^{14}	$\underline{P}15$	S^{16}	Cl^{17}
Cu^{29}	$\boldsymbol{Ca^{20}}$	$\underline{Ga}31$	Ge^{32}	As^{33}	$\boldsymbol{Se^{34}}$	Br^{35}
Ag^{47}	$\boldsymbol{Zn^{30}}$	In^{49}	Sn^{50}	Sb^{51}	Te^{52}	I^{53}
Au^{79}	Cd^{48}	Ti^{81}	Pb^{82}	$\underline{Bi}83$	Po^{84}	At^{85}
	Hg^{80}					

***Table I.2**. Selected Portions of Mendeleev's Periodic Table*

The atomic electronic configuration and atomic number of the atoms constituting the compounds studied are shown in Table (I-3).

The element	**Atomic number (Z)**	**Electronic Configuration**
Ca	20	**[Ar]** $4s^2$
Se	34	**[Ar]** $3d^{10}\ 4s^2\ 4p^2$
Zn	30	**[Ar]** $3d^{10}\ 4s^2$

***Table I.3.** Atomic number and electronic configuration of the elements studied.*

Element II provides 2 valence electrons (from an s orbital) and element VI provides 6 (2 from an s orbital and 4 from a p orbital), making 8 electrons for each element pair, as is the case for all semiconductors (IV-IV, III-V, II-VI). The atomic orbitals then hybridize to form sp3 interatomic bonds, where each cation (element II) is in a tetrahedral environment of an anion (element VI) and vice versa. These bonds are polar, with a character intermediate between ionic and covalent bonds **[6]**. Qualitatively, group VI elements are more electronegative than group II elements.

I.4.3. Crystallographic Structure of the Binary Compounds CaSe and ZnSe

I.4.3.1. Description of the rock-salt NaCl structure (CaSe)

The NaCl structure is represented by two face-centered cubic's offset from each other by a quarter of the cube diagonal, this is shown in Figure (I.4). The group space is Fm3men (Hermann-Mauguin notation) **[9]** with the number "225" in the International Tables of Crystallography.

The atoms occupy the positions:

Cl :(0, 0,0);(½, ½,0);(½, 0,½); (0,½, ½).

Na :(½,½,½);(0, 0,½);(0, ½,0);(½, 0.0).

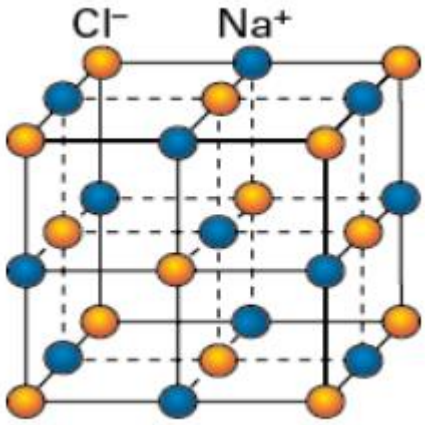

Figure I.4. *NaCl crystal structure*

I.4.3.2. Description of the Zinc Blende structure (ZnSe)

The compound ZnSe crystallize in the so-called Zinc Blende (or sphalerite) structure shown in Figure (I.5), which is similar to the diamond structure. This structure consists of two face-centered cubic (FCC) sublattices: one formed by zinc (Zn) atoms and the other by selenium (Se) atoms, shifted relative to each other by one quarter of the main diagonal of the unit cube. Each atom is located at the center of a regular tetrahedron whose vertices are occupied by atoms of the opposite species. The structure is fully defined by the lattice constant **a**, also called the lattice parameter. This crystalline arrangement gives ZnSe its characteristic semiconductor properties **[10].**

The atomic positions are **[11–12]**:

Zn: (0, 0, 0); (½, ½, 0); (½, 0, ½); (0, ½, ½).

Se: (¼, ¼, ¼); (¼, ¾, ¾); (¾, ¼, ¾); (¾, ¾, ¼).

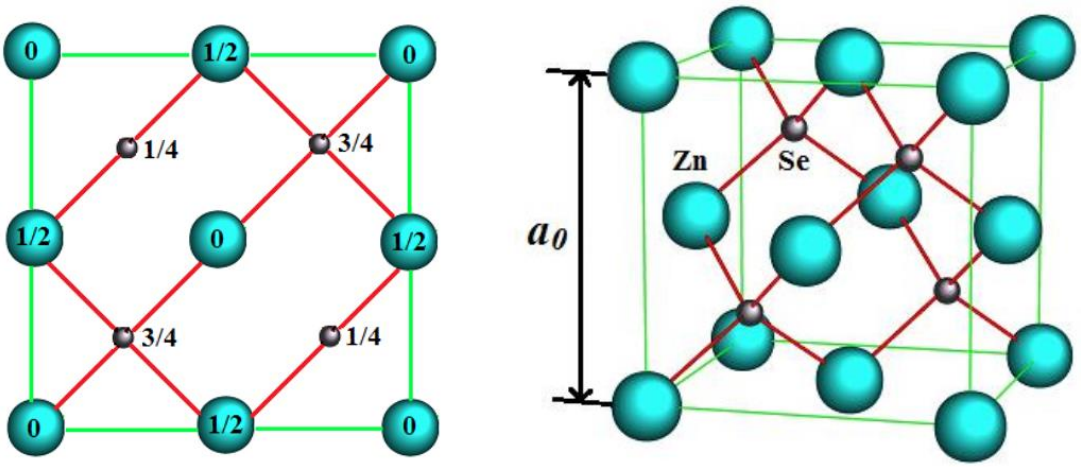

Figure I.5. *Crystal lattice of the Zinc-blende structure.*

The lattice parameters of CaSe and ZnSe in the bulk state are: a = 5.916 Å **[13]** and a =5.668 Å **[14]** respectively

I. 5. First Brillouin zone

By definition, the primitive Wiigner-Seitz cell of the reciprocal lattice is called the first Brillouin zone. The terms Wigner-Seitz cell and first Brillouin zone refer to identical geometric constructions. In practice, the first Brillouin zone is only applied to the cell of the k-space **[15]**. It has the shape of a truncated octahedron; this reduced space of the reciprocal lattice is characterized by points and lines of particular importance, called points and lines of high symmetry. This information for both structures is shown in Figure (1.6).

I. 5. 1. Points of high symmetry:

The high symmetry points are the intersection points of each of the high symmetry lines with the boundaries of the first Brillouin zone. These points are denoted by:

Γ, K, X, L, W, and Z with the following meanings:

Γ: This point occupies the central position of the first Brillouin zone and is characterized by the coordinates; $k_{\Gamma} = (0,0,0)$

X: This point is located at the center of a square face of the octahedron associated with one of the axes; k_x,k_yOr k_z. In othersterms, with eachsquare faces, we haveso:

$$k_x = \frac{2\pi}{a}(\pm 1,0,0), \qquad k_y = \frac{2\pi}{a}(0,\pm 1,0), \qquad k_z = \frac{2\pi}{a}(0,0,\pm 1)$$

L: This point occupies the central position of a hexagonal face of the octahedron, characterized by the coordinates: $k_l = \frac{2\pi}{a}(1,1,1)$

W: This point is located at one of the vertices of the square faces, with the coordinates: $k_w = \frac{2\pi}{a}\left(0,\frac{1}{2},1\right)$

Z: This point is positioned along the line connecting the center of a square face to one of the corners of the octahedron, with the coordinates: $k_z = \frac{2\pi}{a}\left(1,\frac{1}{2},1\right)$

I. 5. 2. Lines of high symmetry

The high symmetry lines are denoted Δ, ∑, and Λ, such that:

Δ: This line illustrates the trajectory or direction<100>. It connects the center Γ to the pointX.

∑: This is a point belonging to the symmetry plane k_x=k_y or k_y=k_z or k_x=k_z

Λ:This line corresponds to the <100> direction. It establishes the connection between the center of the zone (Γ) and the center of a hexagonal face, represented by the point L of the octahedron.

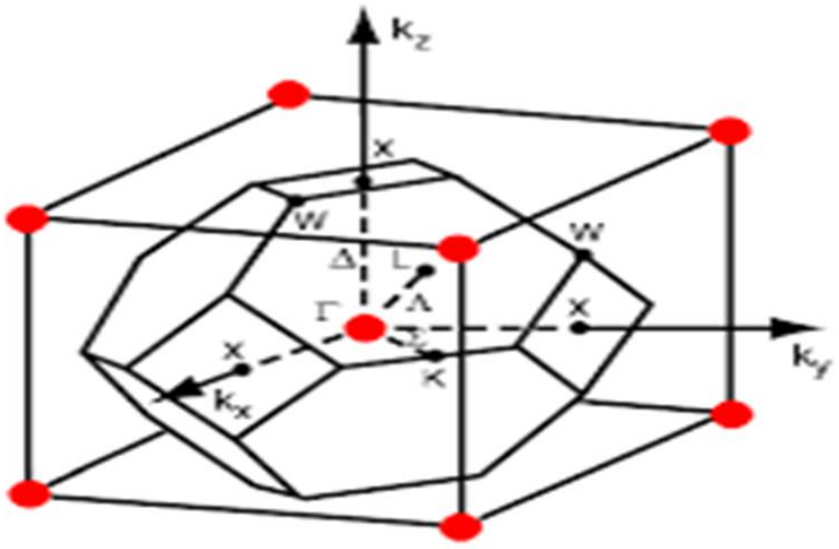

Figure I.6.*First Brillouin Zone (zinc-blende, NaCl) with the representation of points and lines of high symmetries* **[16]**

I. 6. Previous work on the study compounds

Numerous theoretical and computational studies have been dedicated to investigating and understanding the structural, electronic, elastic, and optical properties etc… of the CaSe and ZnSe compounds, which belong to the family of II–VI semiconductors**.** The significance of these materials lies in their excellent physical characteristics, such as mechanical stability**,** high hardness**,** good thermal conductivity, and their electronic and optical behavior under conditions of elevated pressure or temperature**.**

I. 6.1. Compound CaSe

Pankaj Kumar et al. (2020) **[17]** explored the structural, mechanical, and optical properties of hexagonal 2D CaSe monolayers using PAW-PBE within DFT. They found the material to be dynamically and thermally stable, exhibiting an indirect band gap of ~2.96 eV and anisotropic optical behavior, including low reflectivity and strong transparency in the visible/UV range. This makes 2D CaSe a candidate for transparent optoelectronic devices and anti-reflective coatings.

Recent theoretical investigations by Khaldi et al. (2024) **[18]** focused on the structural and elastic properties of calcium chalcogenides (CaS, CaSe, and CaTe) under hydrostatic pressure using DFT within the GGA approximation. They reported that CaSe crystallizes in the rock-salt (B1) structure and maintains mechanical stability under increasing pressure, as confirmed by the positive elastic constants satisfying Born's criteria. Moreover, the study predicted a pressure-induced phase transition from the B1 to the B2 (CsCl-type) structure at approximately 25.2 GPa. The compound also exhibited a high bulk modulus and low compressibility, suggesting strong resistance to deformation and potential applicability in high-pressure environments.

In a recent study by Chauhan et al. (2025) **[19]**, the temperature-dependent mechanical and thermal properties of CaSe were thoroughly investigated using first-principles DFT methods and Born stability criteria. The study explored a wide range of parameters including second- and third-order elastic constants, ultrasonic velocities, Debye temperatures, specific heat, and thermal conductivity across temperatures up to 500 K. The results confirmed the mechanical

stability and brittleness of CaSe and highlighted its potential in high-temperature applications due to its robust acoustic and thermal characteristics.

I. 6.2. Compound ZnSe

In an earlier work, Khenata et al. (2006) **[20]** performed a detailed DFT-LDA analysis of the structural, elastic, and electronic properties of ZnSe in the zinc blende (B3) phase. Using the FP-LAPW method implemented in WIEN2k, the authors calculated fundamental properties such as the lattice constants, elastic constants (C_{11}, C_{12}, C_{44}), bulk modulus, and band gap evolution under pressure. A key finding was the direct band gap at the Γ point, which makes ZnSe a strong candidate for optoelectronic applications. Moreover, the study revealed how pressure influences its electronic structure and optical behavior, emphasizing the material's stability and versatility under extreme conditions.

In another study, Ghaleb et al. (2024) **[21]** investigated the structural, electronic, and optical properties of ZnSe in its zinc-blende (cubic sphalerite) phase using first-principles calculations based on both LDA and GGA approximations. They found that ZnSe possesses a direct band gap of approximately 1.33–1.34 eV at the Γ-point, making it a promising candidate for optoelectronic devices. The study also revealed robust optical characteristics, including a high refractive index and strong ultraviolet absorption, which confirm the material's suitability for applications such as UV detectors and photovoltaic systems**.** The mechanical stability was also confirmed through consistent elastic constants.

References

[1] Boucenna, S., Mémoire en physique du solide, Université Ferhat Abbas, Sétif, (2010).

[2] Labidi, S., Meradji, H., Labidi, M., Ghemid, S., Drablia, S., and El Haj Hassan F., First principles calculations of structural, electronic and thermodynamic properties of SrS, SrSe, SrTe compounds and SrS1-xSex alloy, Phys. Procedia, 2, 1205-1212, (2009).

[3] Imajuku, W., and Takahashi, M., J. Appl. Phys.34, (1995).

[4] Boudouani, M. S., Mémoire de master, Université Abou BekrBelkaid, (2017).

[5] YuboZhanga,Xun Yuan, XiudongSunaWenqingZhang,Solid State Communications 152 (2012) 588-592

[6] Arnoult, A., Thèse de doctorat université Joseph Fourier, Grenoble I, (1998). [7] Ferreira, B., Thèse de doctorat, Université de Bordeaux I, (2002).

[8] Kiréev, P. La physique des semi-conducteurs. Ed. Mir, Moscow, (1975).

[9] Transformation in crystallography –H .ARNOLD-InternationaleTables for crystallography –Volume A.55.

[10] Louazani Ahmed. « Etudes des propriétés structurales, élastiques et électroniques, semi conducteur III-V GaAs, InP», Université Dr. Tahar Moulay de Saida(2015).

[11] Refice Fatima Zohra, Mémoire de master, «Etude théorique des propriétés électronique Optiques et diélectriques des alliages semi-conducteurs», Université Mohamed Boudiaf-Msila, (2017).

[12] Belmadi Mohamed, Mémoire de master, «Technologie et intégration en semi-conducteurs III-V», Université Mouloud Mammeri De Tizi-Ouzou, (2016).

[13] H. Luo , R. G. Greene , K. G. Handehari , T. Li and A. L. Ruoff, Phys. Rev. B 50, 16232 (1994).

[14] H. Okuyama, Y. Kishita, and A. Ishibashi, Phys. Rev. B 57, (1998) 2257.

[15] N. W. Ashcroft, N.DavidMermin, physique des solides, édition originale SaaundersCollegePublisbing(1976).

[16] C. Kittel. Introduction to solid state physics, Dunode (1972).

[17] Pankaj Kumar et al. (*2020)* – "DFT investigation on the optical properties of 2D-CaSe" AIP Conf. Proc. 2265, 030496.

[18] Khaldi, A., Bouarissa, N., & Labidi, S. (2024). Pressure influence on structural parameters and elastic properties of rock-salt CaX (X = S, Se and Te) materials. Chemical Physics Impact, 6, 100237.

[19] Chauhan, J., Singh, D., Khenata, R.**,** Meradji, H., Bin-Omran, S., & Maddheshiya, A. K. (2025). Temperature-dependent elastic, mechanical, thermal, and acoustic behavior in alkaline earth semiconductors CaX (X = S, Se, Te). Zeitschrift für Naturforschung A.

[20] Khenata, R., Bouhemadou, A., Sahnoun, M., et al. *(2006)*. Structural, electronic and optical properties of ZnSe under pressure. Physica B: Condensed Matter, *373(1), 99–107*

[21] Ghaleb, A. M., Al-Anazi, A. M., Qaid, M. M., & Alduais, N. A. (2024). Structural, electronic, and optical properties investigation of ZnSe cubic sphalerite compounds using density functional theory (DFT). Problems of Atomic Science and Technology, 1(149), 59–65.

Chapter II

Theoretical notions and calculation methods

II.1. Introduction

The physics of materials and condensed matter science are closely linked to the understanding and utilization of systems of interacting electrons and nuclei. In theory, all characteristics of materials can be identified if we have powerful computational tools to solve this quantum mechanical problem. In practice, studying electronic properties provides information on structural, electronic, mechanical, thermal, vibrational, and optical properties. However, the electrons and nuclei that make up materials form a strongly interacting many-body system, which makes direct solution of the Schrödinger equation impossible **[1].** The foundations of density functional theory are presented in this chapter.

II.2. Schrödinger Equation

Each crystalline body can be considered a unique system composed of light particles (electrons) and heavy particles (nuclei) **[2]**. In non-relativistic quantum mechanics, all information is contained in the wave function, whose evolution is governed by the Schrödinger equation, also known as the time-dependent equation, which is written as follows:

$$H|\Psi\rangle = E|\Psi\rangle \quad \textbf{(II.1)}$$

H is the Hamiltonian of the system, which includes the kinetic and potential energy, and it is expressed in the following form:

$$\mathrm{H_{tot}} = \mathrm{T_e} + \mathrm{T_n} + \mathrm{V_{n-e}} + \mathrm{V_{e-e}} + \mathrm{V_{n-n}} \quad \textbf{(II.2)}$$

$$H = -\frac{1}{2}\sum_i \nabla_i^2 - \frac{1}{2}\sum_A \frac{\nabla_A^2}{M_A} - \sum_i \sum_A \frac{Z_A}{R_{Ai}} + \sum_{i<j} \frac{1}{r_{ij}} + \sum_{A<B} \frac{Z_A Z_B}{R_{AB}} \quad \textbf{(II.3)}$$

The equations used in this manuscript are expressed in atomic units (a.u.)

$$(\hbar^2 = e^2 = m = \hbar\pi\varepsilon_0 = 1). \quad \textbf{(II.4)}$$

$Te = -\frac{1}{2}\sum_i \nabla_i^2$ is the kinetic energy of the electron **(II.5)**

$T_n = -\frac{1}{2}\sum_A \frac{\nabla_A^2}{M_A}$ is the kinetic energy of the nuclei **(II.6)**

$V_{ne} = -\sum_i \sum_A \frac{Z_A}{R_{Ai}}$ is the potential energy of attraction between nuclei and electrons. **(II.7)**

$V_{ee} = \sum_{i<j} \frac{1}{r_{ij}}$ is the potential energy of repulsion between the electrons. **(II.8)**

$V_{nn} = \sum_{A<B} \frac{Z_A Z_B}{R_{AB}}$ is the potential energy of repulsion between nuclei. **(II.9)**

The i and j represent the electrons, while the A and B represent the nuclei. MA and ZA represent respectively the mass and charge of the nucleus in question, while RAi, rij, and RAB represent respectively the distances between the nucleus and the electron, the electron/electron, and the nucleus/nucleus.

II.3. Fundamental Approximations

II.3.1. Born-Oppenheimer Approximation

This approximation was jointly developed; however, given the complexity of equation (III-1), it is impossible to solve it even in the simplest case. It is an N-body problem that can only be solved using approximations.

r Born and Oppenheimer in 1927 **[3]**. It involves taking into account the large mass disparity between the nuclei and the electrons **[4]**.

The first observation is that the duration of the motion of nucleons is often shorter than that of electrons. In reality, electrons have a lower mass than protons, approximately 1 for 1836, which means their speed is higher. In this perspective, it was suggested in the early days of quantum mechanics that electrons can be described by immediately following the motion of nucleons, always in the same stationary state of the initial electronic Hamiltonian.

Thus, the total Hamiltonian is **[5]**:

$$H_T = T_e + V_{n-e} + V_{e-e} \quad \textbf{(II.10)}$$

The Born-Oppenheimer approximation is called adiabatic because it allows distinguishing the electronic problem from that of lattice vibrations. Thus, we can write the wave function of the system, which is the solution of the Schrödinger equation in the adiabatic approximation, as follows:

$$\psi(R,r) = \psi_n(R).\psi_e(r) \quad \textbf{(II.11)}$$

With : Ψn the nuclear wave function is Ψe is the electronic wave function

II.3.2. The Hartree and Hartree-Fock Approximations:

The first approach to the multi-electron problem can be likened to Hartree's initial proposal **[6]** (1928). The fundamental idea is that the multi-electron wave function can be represented

as a simple product of single-electron orbitals, which is why this approximation is also known as the orbital approximation. Even though it is generally not real for electronic systems, it is simply meant to illustrate the aspect of the one-electron approach.

$$\Psi(\overrightarrow{r_1},\ \overrightarrow{r_2} \dots, \overrightarrow{r_n}) = \Psi_1(\overrightarrow{r_1})\Psi_2(\overrightarrow{r_2}) \dots . \Psi_n(\overrightarrow{r_n}) \quad \textbf{(II.12)}$$

The free electron hypothesis is used for the latter, which means it does not take into account the interactions between electrons and spin states. This leads to two major repercussions: We overestimate the total Coulomb repulsion Ve-e of the electronic system.

The Pauli exclusion principle is not taken into consideration.
Fock created the Hartree model in 1930 and introduced a spin principle in the field of electronics. Therefore, there is N! probability of placing N electrons at the position r $\vec{r}_N, \dots\dots\dots\dots\dots \vec{r}_1, \vec{r}_2$ **[7-8]**. For example, the first possibility is:

$$\boldsymbol{\Psi_1(r_1).\Psi_2(r_2)\Psi_3(r_3)} \dots \dots \dots \dots \dots \ \boldsymbol{\Psi_n(r_n)} \quad \textbf{(II.13)}$$

The second possibility is:

$$\boldsymbol{\Psi_1(r_1).\Psi_2(r_3)\Psi_3(r_2)} \dots \dots \dots \dots \dots \ \boldsymbol{\Psi_n(r_n)} \quad \textbf{(II.14)}$$

By using all the substitutions, we obtain N! End in the same type, which is a more serious consequence than the first. To correct this defect, Fock [9] suggested the Pauli exclusion principle. Thus, the electronic wave function is written in the form of a Slater determinant composed of a single-electron spin orbital that respects the antisymmetry of the wave function.

$$\Psi^{HF}(r_1,\ r_2, \dots \dots r_n) = \frac{1}{\sqrt{N!}} \begin{vmatrix} \Psi_1(r_1).\Psi_2(r_2) \dots . \dots \dots . . \Psi_n(r_n) \\ \Psi_1(r_n).\Psi_2(r_n) \dots . \quad \dots \dots . \Psi_n(r_n) \end{vmatrix} \quad \textbf{(II.15)}$$

Or: $1/\sqrt{N!}$ is the normalization factor.
This is an estimate from Hartree Fock 1930.
Despite the precise description of the electronic system thanks to the Slater determinant, which takes into account the Pauli principle, the Hartree-Fock method remains complex. The calculation is still very complex numerically. The modern and certainly more powerful method used by researchers is the density functional method. This method has significantly simplified the calculations initially.

II.3.3. Density Functional Theory (DFT)

II.3.3.1. Problem Statement

Density Functional Theory (DFT) is a quantum calculation tool that allows for the study of electronic structure, in principle, with precision. At the beginning of the 21st century, it is one of the most commonly used methods in quantum calculations, both in quantum chemistry and condensed matter physics, for systems of very diverse sizes, ranging from a few atoms to several hundred **[10]**.

The multi-electron wave function is the basis of classical methods in theories of the electronic structure of matter, notably Hartree-Fock theory and methods derived from this formalism. Density functional theory primarily aims to replace the multi-electron wave function with the electron density as the fundamental quantity for calculations.
The DFT model is derived from the work of Llewellyn Thomas and Enrico Fermi in the late 1920s. However, the theoretical formalism on which the current method is based will not be established until the mid-1960s, with contributions from Pierre Hohenberg, Walter Kohn, and Lu Sham.

II.3.3.2. Hohenberg-Kohn Theorems

The basic principle of DFT is simply summarized in two theorems, initially introduced by Hohenberg and Kohn **[11]**, which assert that there is a bijection between the set of potentials and that of minimizing densities, based on the following points:
a) The total energy of the ground state of a system consisting of interacting electrons is a distinct characteristic of the density.

$\boldsymbol{E}$ = [($\boldsymbol{r}$)] **(II.16)**

b) Par conséquent, obtenir la densité qui réduit l'énergie liée à l'Hamiltonien permet d'évaluer l'énergie de l'état fondamental du système.
Le deuxième théorème de Hohenberg et Kohn insiste sur le fait que la densité qui réduit l'énergie est celle de l'état fondamental.

($\boldsymbol{\rho_0}$) = ($\boldsymbol{\rho}$) **(II.17)**

$\boldsymbol{\rho_0}$: The density of the ground state
The functional of the total energy of the ground state is written as follows:

$$\boldsymbol{E}\left[\boldsymbol{\rho}(\overrightarrow{\boldsymbol{r}})\right] = \boldsymbol{F}\left[\boldsymbol{\rho}(\overrightarrow{\boldsymbol{r}})\right] + \int \boldsymbol{V_{ext}}\,(\overrightarrow{\boldsymbol{r}})\,\boldsymbol{\rho}(\overrightarrow{\boldsymbol{r}})\boldsymbol{d^3}\overrightarrow{\boldsymbol{r}} \quad \textbf{(II.18)}$$

Où: $\boldsymbol{F[\rho(\vec{r})] = \langle \Psi | T + V | \Psi \rangle}$ **(II.19)**

Let's emphasize that the functional F[ρ] is universal for any multi-electron system. If the functional F[ρ] is known, then it will be relatively easy to use the vibrational principle to determine the total energy and the electronic density of the ground state for a given external potential. Alas, the Hohenberg-Kohn theorem provides no indication about the form of F[ρ].

II.3.3.3. Kohn and Sham Approach

Density functional theory remains today the most commonly used method for calculating electronic structure. Its success is attributed to the approach proposed by Kohn and Sham (KS) [12] in 1965. The objective of this method is to identify the precise characteristics of a multi-particle system based on multi-particle methods. In practice, this revolution in the field has led to some approximations that have been very satisfactory.

The expressions for the kinetic energy and potential energy for this fictitious system are known, which is of interest. It is therefore possible to transition from a problem with a wave function Ψ(r) for Ne electrons to a problem with Ne single-electron wave functions ϕ(r), called Kohn-Sham states. We denote T_int [ρ] as the kinetic energy of the system of Ne independent electrons and V_int [ρ] as the classical potential energy, which is the Hartree term:

$$\boldsymbol{V_{ind}[\rho] = \frac{1}{2} \int \frac{\rho(r)\rho(r')}{|r-r'|} dr dr'} \quad \textbf{(II.20)}$$

The value of the system's energy is therefore precise:

$$\boldsymbol{E[\rho] = T_{ind}[\rho] + V_{ind}[\rho] + E_{xc}[\rho] + \int V_{e-n}(r)\rho(r)dr} \quad \textbf{(II.21)}$$

Et : $\boldsymbol{F_{HF} = T_{ind}[\rho] + V_{ind}[\rho] + E_{xc}[\rho]}$ **(II.22)**

With: $\boldsymbol{E_{xc}[\rho]}$ is The exchange-correlation energy functional encompasses all the complex and intricate concepts of the system, namely the correlation effects caused by the quantum nature of electrons. This expression encompasses all multielectronic effects.

$$\boldsymbol{E_{xc}[\rho] = T[\rho] - T_{ind}[\rho] + V[\rho] - V_{ind}[\rho]} \quad \textbf{(II.23)}$$

By defining this new functional, Kohn and Sham had the idea to gather as much information as possible on the kinetic and potential terms, to group everything that is unknown into a single contribution that can be approximated, in order to reduce the error on the total energy. By reducing (II.11), we obtain the Euler equation.

$$\int \left[\frac{\delta T_{ind}[\rho]}{\delta \rho(r)} + \int \frac{\rho(r'(dr'')}{|r-r'|} + V_{e-n}(r) + \frac{\delta E_{xc}[\rho]}{\delta \rho(r)}\right] \delta\rho(r)dr = 0 \quad \textbf{(II.24)}$$

If the number of particles remains constant, we obtain:

$$\int \delta\rho(r)dr = 0 \quad \textbf{(II.25)}$$

In equation (II.22), the term in parentheses thus remains constant. The first Kohn-Sham equation thus allows us to define an effective potential in which the electrons are found.

$$V_{eff}[\rho(r)] = V_{e-n}(r) + V_{Hartree}(r) + V_{xc}[\rho(r)] \quad \textbf{(II.26)}$$

The Hartree potential is defined as follows:

$$V_{Hartree}(r) = c\int \frac{\rho(r')dr'}{|r-r'|} dr' \quad \textbf{(II.27)}$$

Taking into account the potential for exchange and correlation:

$$V_{xc} = \frac{\delta E_{xc}[\rho]}{\delta \rho(r)} \quad \textbf{(II.28)}$$

The second Kohn-Sham equation, known as (II.22) and (II.24), is the system of Ne single-electron Schrödinger equations that allows for the determination of the Ne states. Kohn Sham $\phi_i(r)$:

$$\left[-\frac{\mathrm{h}^2}{2m_e}\vec{\nabla}^2 + V_{eff}(\vec{r})\right]\phi_i(r) = \varepsilon_i\phi_i(r), \quad i = 1, \dots, N \quad \textbf{(II.29)}$$

With ε_i the Kohn-Sham energies. Having these states, all that remains is to determine the electronic density of the system. The third Kohn-Sham equation is as follows:

$$\rho(r) = \sum_{i=1}^{N_e}|\phi_i(r)|^2 \quad \textbf{(II.30)}$$

It is necessary to solve these three interdependent equations self-consistently to obtain the ground state density. The iterative solution of these three equations is the basis of all type calculations. DFT It is important to emphasize that in DFT, only the total energy, the Fermi energy, and the electron density have physical significance.
The Kohn-Sham states and energies are just computational tools. The DFT method is currently an accurate method, it is used in numerous scientific works to calculate certain quantities such as band structures.

When the electrons are loosely bound, the Kohn-Sham states provide a good approximation of the function Ψ_ede Ne electrons of the System**[13]**.

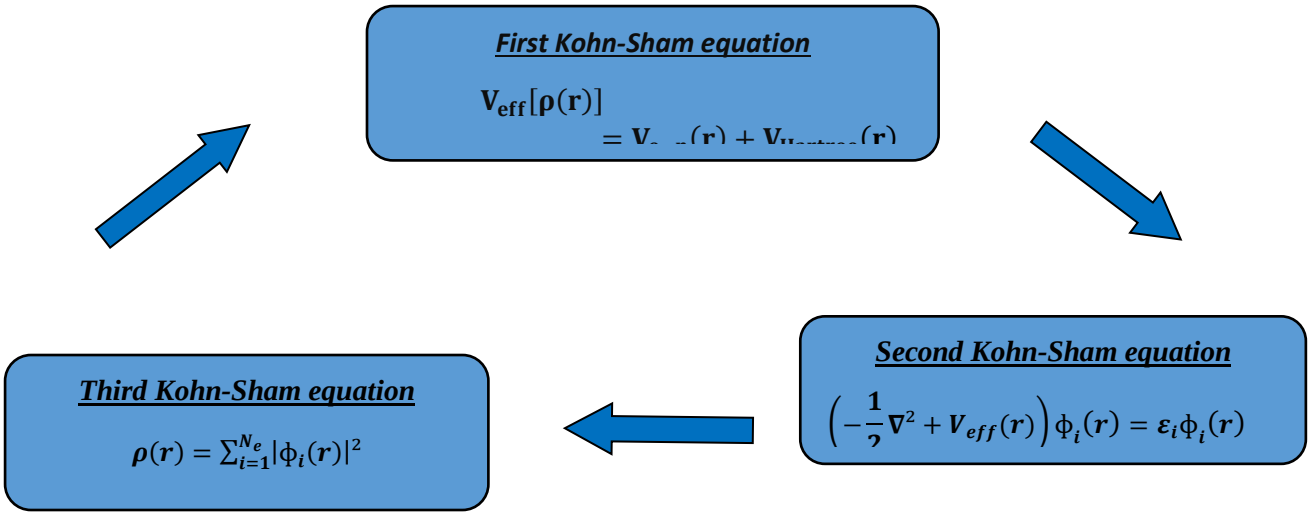

Figure II.*1. Interdependence of the Kohn-Sham equations* ***[14]***

II.3.3.4. The exchange-correlation functional

The exchange-correlation term is the only ambiguity in the Kohn-Sham (KS) approach. The difficulty in solving the KS equations lies in their formal complexity. However, this functional can be subjected to local or semi-local density approximations, that is, the Exc energy. So, to calculate the exchange and correlation energy and potential, several approximations are used, the main ones being LDA and GGA. These estimations have piqued the interest of many researchers and led to significant advancements in this field.

a-Local Density Approximation (LDA)

Kohn and Sham introduced the local density approximation (LDA) approach in 1965. The idea is to assume that the electronic density varies slowly within the system, without taking into account the impact of local variations in electronic density on the exchange and correlation energy **[15]**:

$$E_{xc}^{LDA}(\rho) = \int \rho(r)\varepsilon_{xc}\big(\rho(r)\big)dr^3 \qquad \textbf{(II.31)}$$

Based on the principle of spin-orbit coupling, you express the exchange-correlation energy as:

$$E_{xc}^{LDA}(\rho\uparrow,\rho\downarrow) = \int \rho(r)\varepsilon_{xc}\,(\rho\uparrow(r),\rho\downarrow(r))dr^3 \qquad \textbf{(II.32)}$$

Taking into account the division of exchange-correlation energy into two parts:

$$\boldsymbol{\varepsilon_{xc}(\rho) = \varepsilon_x(\rho) + \varepsilon_c(\rho)} \quad \textbf{(II.33)}$$

With: $\boldsymbol{\varepsilon_c}$and $\boldsymbol{\varepsilon_x}$: they represent the correlation energy and the exchange energy, respectively. The calculation of the electron density depends on all the occupied orbits, that is to say:

$$\rho(r) = \sum \mathbf{\Psi}_i^* (r)\mathbf{\Psi_i}(\mathbf{r}) \quad \textbf{(II.34)}$$

The local density approximation (LDA) method provides good results for systems where the density fluctuates slowly. Systems with more inhomogeneous density exhibit lower performance, which has led to numerous developments aimed at improving the obtained results.

b- Approximation of the generalized gradient GGA

Another method to improve the local density approximation, which makes the Exc energy dependent on the density gradient ρ(r), is the generalized gradient approximation. The GGA method (Generalized Gradient Approximation) is extremely effective, as it often allows for a better description of bonding, resulting in improved total energy results and enhanced geometries for weak bonds. The LDA approach is less effective than this method for systems with inhomogeneous densities.

The GGA represents the exchange and correlation energy as follows:

$$\boldsymbol{E_{xc}^{LDA}(\rho) = \int f[\rho(r)\big(\rho(r), \nabla\rho(r)\big)dr^3} \quad \textbf{(II.35)}$$

$\boldsymbol{\nabla\rho(r)}$: expresses the gradient of the electronic density.

c- mBJ Potential

The exchange potential was first introduced by Back and Johnson in 2006. In 2009 **[16]**. **[17]**. Tran and Blaha published what they called the mBJ potential, also known as the "Beck Johnson modification," which has been implemented in the latest version of the Wien2k code. These same authors **[18]** also experimented with the exchange potential suggested by Beck and Johnson (BJ 2006). They found that the use of the BJ potential associated with the LDA correlation potential always results in underestimated values of the band gap energies.

An original modification of the simple BJ potential was proposed by Tran and Blaha [2009] and was well accepted by other more costly approaches such as the hybrid functional **[19-20]** and the GW method **[21-22]**.

The following formula gives the modified potential (mBJ) of Tran and Blaha **[23]**:

$$vV_{x,\sigma}^{mbj}(r) = cV_{x,\sigma}^{BR}(r) + (3c-2)\frac{1}{\pi}\sqrt{\frac{5}{12}}\sqrt{\frac{2t_\sigma(r)}{\rho_\sigma(r)}} \quad \textbf{(II.36)}$$

$$\rho(r) = \sum_{i=1}^{n\,\sigma}|\Psi i,\sigma(r)|^2 \quad \textbf{(II.37)}$$

ρ is the electron density

$$t_\sigma(r)\frac{1}{2}\sum_{i=1}^{n_\sigma}\nabla\Psi_{i,\sigma}^{+}(r)\nabla\Psi_{i,\sigma}(r) \quad \textbf{(II.38)}$$

The density of kinetic energy represented by the index σ is the spin notation.

II.3.3.5. Solution of the Kohn-Sham Equations

The solution of the Kohn-Sham equations requires the choice of a basis for the wave functions, which can be considered as a linear combination of orbitals, known as Kohn-Sham (KS) orbitals.

$$\psi_i\left(\vec{r}\right) = \sum C_{ij}\phi_j\left(\vec{r}\right) \quad \textbf{(II.39)}$$

$\phi_\alpha(r)$ and $C_{i\alpha}$ are The basis functions and the development coefficients are respectively the basis functions.

When the orbitals are occupied, it reduces the total energy. The simplified calculation of symmetry points in the first Brillouin zone is facilitated by the solution of the Kohn and Sham equations. It is an iterative solution that uses a self-consistent iteration cycle, as shown in the flowchart Figure (II.2).

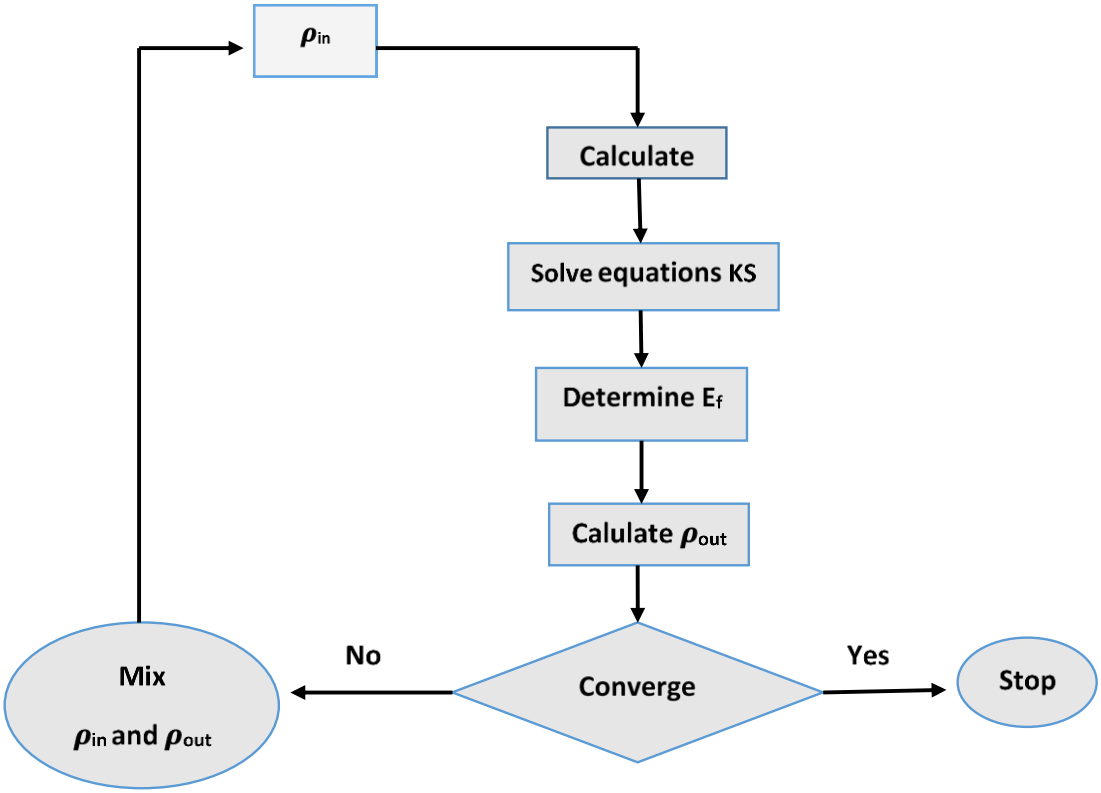

Figure II.2.*Diagram of the self-consistent calculation of Density Functional Theory*

II.4. Augmented and Linearized Plane Wave Method (FP-LAPW)

The FP-LAPW method is an improved version of the LAPW method; it is a method for solving the Poisson equation that allows for the calculation of the corresponding correlation potential.

This method ensures the continuity of the potential at the surface of the defined Muffin Tin sphere (M,T) by using the derivative of $\dot{U}(\vec{r})$, $Y_{lm}(\vec{r}\dot{U}(r\ \vec{})$, Y_lm (r $\vec{}$) with respect to energy **[24]:**

$$\varphi(\vec{r}) = \begin{cases} \frac{1}{\Omega^{\frac{1}{2}}} \sum_{G} C_G e^{i(G+K)rr > R_\alpha} \\ \sum_{lm} A_{lm}\, Ul(\vec{r}) + B_{lm} Ul(\vec{r}) Y_{lm}(\vec{r}) \qquad r < R_\alpha \end{cases} \qquad \textbf{(II. 40)}$$

The function U_l is known as the function of the (APW) method **[25]**, and the function (r)Y_lm (r)U(r $\vec{}$),Y_l (r $\vec{}$) is subject to the following condition:

$$\left\{-\frac{d^2}{dr^2}+\frac{l(l+1)}{r^2}+\ v\ (\vec{r})-\mathrm{E}_l\ \right\}rU^*_{l(\vec{r})}=\ rU_{l(\vec{r})} \qquad \textbf{(II.41)}$$

Regarding non-relativity, the functions (r) and U_l (r) ensure continuity at the surface of a sphere (M.T). This is the continuity with the plane wave outside. Reduces the function. Its APW function. The main function becomes that of the LAPW method. If the coefficients of the equivalent function are identical to the APWs function, they constitute the only plane wave in the intrusive region.

In the ball, the function is influenced by the APWs function when the energy band E slightly differs from the APWs function. The best APWs radial function is followed by linear arrangements, which implies that the Ul function can propagate over the derived function and the El energy in the following form:

$$\boldsymbol{U_l(E.(E.r)+(E-E_l)U_L(E.r)+0((E-E_L)^2)r)=U_l} \qquad \textbf{(II.42)}$$

$\boldsymbol{0((E-E_l)^2}$ It represents the energy error of the quadrant.

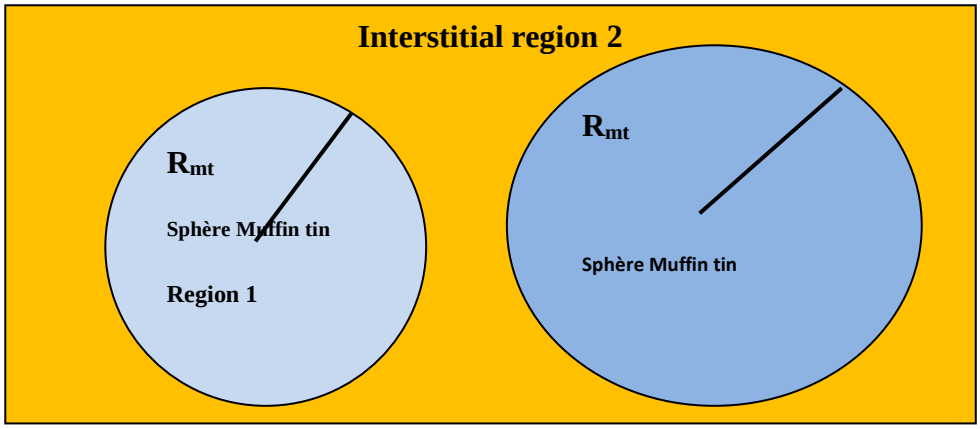

Figure II.3.*Distribution of atomic unit cells adopted in the APW method: muffin-tin* spheres (S) of radius R_{MT} and interstitial region (1).

* Region 1: characterized by atomic spheres of radius R_{MT} (muffin tin).

* Region 2: located outside the spheres and called interstitial region

II.5. THE WIEN2K CODE

Wien2K, simulation code, Institute of Materials Chemistry, Vienna University of Technology, 1990, Blaha P, Schwartz K, Sorintin P. and Trickey S. B **[26]**.

Then, this code has been constantly revised and updated several times. Variants of the original Wien code were created (renamed according to the year of their introduction, Wien93,

Wien95, Wien97...). The Wien2K version (2014) was used by us **[27-28].**

The density of states, the Fermi energy, and the energy bands.

Electrons, spins, and X-ray structure factors.

The total energy, atomic forces, equilibrium structures, and structural optimizations.

The polarization of spins (whether they are ferromagnetic, antiferromagnetic, or otherwise) and the connection between spin and orbit.

The variations in the emission and absorption spectra of X-rays.

The optical characteristics.

II .5.1 Wien2K Algorithm

The diagram below presents the use and operation of the various Wien2K programs Figure (II.4). Initialization is the first step of the calculation, which involves running a series of small auxiliary programs that generate inputs for the main programs **[29]**.

NN: a module that enumerates the distances between the nearest neighbors up to a given limit (usually equal to 2), which allows determining the value of the atomic sphere radius. Thus, it supervises the structure file cas.struct (Atom equivalence).

The output file of this subprogram is cas-outputnn.

SGROUP: allows determining the space group of the structure specified in the cas.struct file. The output file is then cas.struct-sgroup..

SYMMETRY: is a program that lists the symmetry operations of the space group of our structure using the information provided in the cas.struct file (type of lattice, number of atoms composing our material and their positions, etc.). It establishes the chronological group of the different atomic locations as well as the matrices of the corresponding rotation operations.

LSTART: generates atomic densities and evaluates how the different orbitals are treated in the band structure calculation (i.e., core states and valence states, with or without local orbitals...). Furthermore, this program requires the cut-off energy that separates core states from valence states, generally set at -6.0 Ry.

KGEN: creates a k mesh in the Brillouin zone. The number of k points is indicated in the first Brillouin zone.

DSTART: creates an initial density for the SCF cycle (self-consistent cycle) by superimposing the atomic densities generated in the LSTART subroutine.

II .5.2.The SCF calculation

The SCF cycle consists of the following steps:

LAPW0: produces the potential using the density.

LAPW1: involves evaluating the valence bands (the eigenvalues and the eigenvectors).

LAPW2: allows the determination of valence densities using eigenvectors.

LCORE: allows determining core states and densities.

MIXER: combines the valence and core densities to generate a new density.

II .5.3 Calculation of properties

The physical properties are calculated using programs:

OPTIMISE: determines the total energy as a function of the volume, which is used to calculate the lattice parameter, the compressibility modulus, and its derivative.

TETRA: calculates the total and partial density of states.

SPAGHETTI: calculates the band structure using the eigenvalues generated by LAPW1.

OPTIC: calculates the optical properties.

XSPEC: calculates the structures of the X-ray absorption and emission spectra

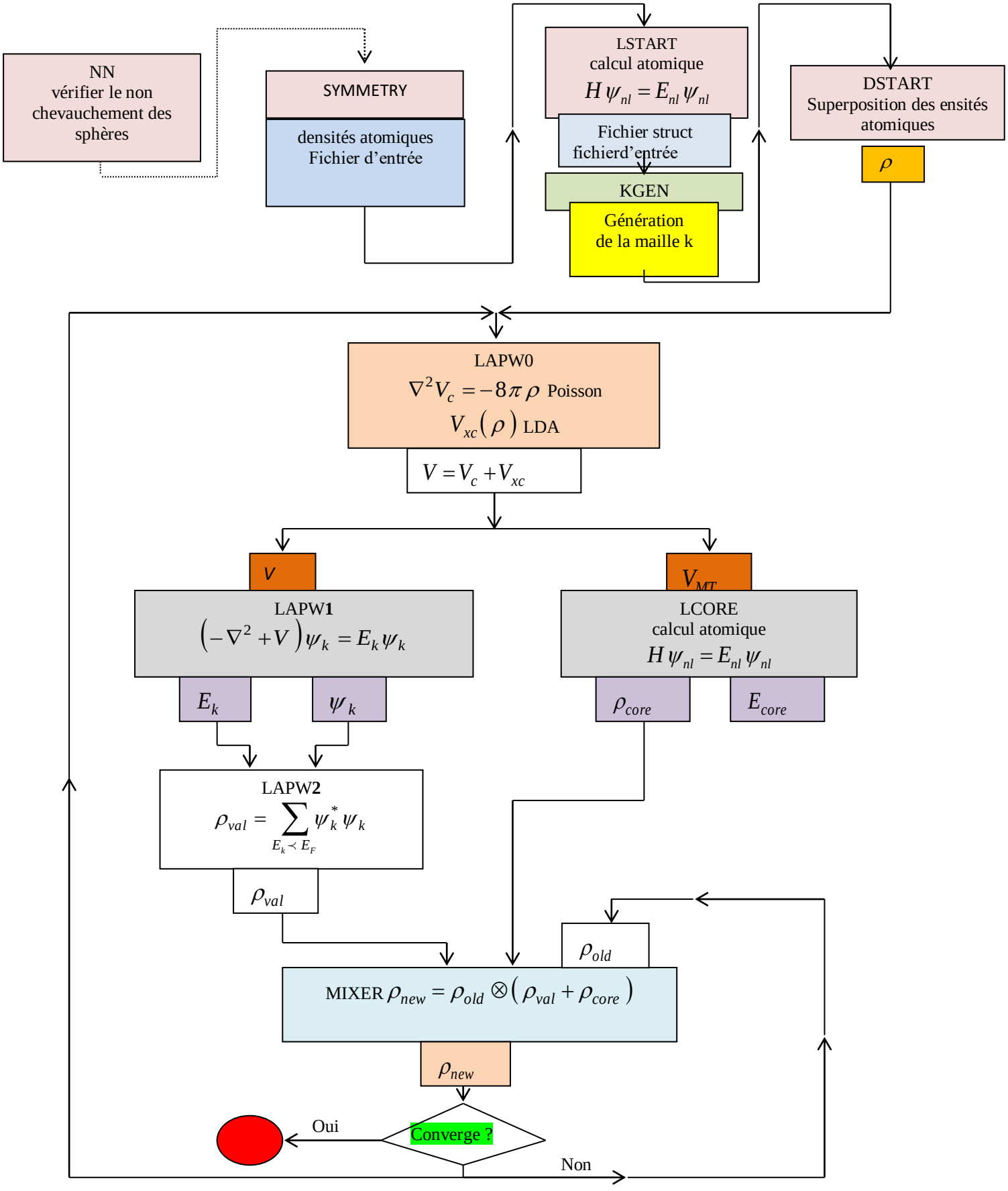

Figure. II.4. .*Wien2k code* ***[30]****.*

_Reference

1].P.A.M. Dirac, proc. Roy. Soc. (Londres), 123, 714 (1929).
[2].I.2. L'équation de Schrödinger d'un solide cristallin http://dspace.univ-msila.dz › bitstream › handle
[3].M.Born,J.R.Oppenheimer,Ann. Phys.87;457(1927).
[4]. Mr BELDJOUDI Karim mémoire de magister « Etude ab-initio des propriétés structurales, élastiques et électroniques des composés XF2 (X=Ca, Ba) sous pression hydrostatique» université FERHAT ABBAS - SETIF (2010)
[5].D.R.Hartree,proc.Cambidgephilos.Soc.24,89(1928)
[6].K. Schwarz, P. Blaha, and S. Trickey, "Electronic structure of solids with WIEN2k,"Molecular Physics, vol. 108, 3147, (2010).
[7]. V. Fock, Z. Phys. 61, 126; 62, 795. (1930) (1930)
[8].N. W. Ashcroft, et N.d .Mermin. Solide state phys. Ed. Holt, Rene hartand Winston Philadelphia, (1976)
[9]. Robert G. Parr et Weitao Yang, *Density Functional Theory of Atoms and Molecules*, Oxford University Press, , 350 p. (ISBN 0195092767) (1989)
[10].P. Hohenberg, and W. Kohn ,"Inhomogeneous electron gas," Phys. Rev. B136:864(1964)
[11].W. Kohn, L. J. Sham, «Self-consistent equations including exchange and correlation effects," Phys. Rev. A140 1133, (1965).
[12]. Samira djouadi; Mémoire de master; «influence de la pression et de la température sur le gap d'énergie des composés AgBr et AgCl »; université badji mokhtar annaba (2017).
[13].A.N. Andriotis, Phys. Rev. B 58, 15300 (1998)
[14].A D. Becke and E R. Johnson, J. Chem. Phys. 124 221101(2006).
[15].F. Tran and P. Blaha , Phys. Rev. Lett. 102**[34].**J. Heyd, J E. Peralta, G E. Scuseria and R L. Martin, J. Chem. Phys. 123 174101(2005).
[16].J. Paier, M. Marsman, K. Hummer, G. Kresse, I C. Gerber and J G. Angyan, J. Chem. Phys. 124 154709(2006).
[17].W G. Aulbur, M. Stadele and A. Gorling, Phys. Rev. B. 62 7121(2000).
[18].S V. Faleev, M V. Schilfgaarde and T. Kotani, Phys. Rev. Lett. 93 126406 (2004).
[19]. Bendaif Samira; thèse de doctorat; «Etude des propriétés structurales, électroniques, thermodynamiques et thermiques des alliages quaternaires $Zn_{1-x}Cd_xS_ySe_{1-y}$», université Badji Mokhtar–Annaba (2015)
[20].J.C. Slater, Phys. Rev. 51, 846(1937)

[21].L. H. Thomas, Pro. Combridge Philos. Soc. 23, 542 (1927).
[22].P. Blaha, K. Schwarz, et J. Luitz, WIEN97. Université technique, Vienna, (1997).
[23]P. Blaha et K. Schwarz, Hyperf. Interagir. 52, 153

(1989).
[24]K. Schwarz, C. Ambrosch-Draxl, et P. Blaha, Phys.
Rev. B 42, 2051 (1990).
[25]B. Winkler, P. Blaha et K. Schwarz, Minéralogiste

[26]B. kohler, P. Ruggerone, S. Wilke, et M. Scheffler,

Phys. Rev. lett. 74, 1387 (1995).

[27]Blaha P., Schwarz K., Sorintin P. et Trickey S. B. dans Comput. Phys. Commun. 59 399. (1990).
[28]P. Blaha, K. Schwarz, G. K. H. Madsen, D. Kvasnicka and J. Luitz, WIEN2K, "AnAugmented Plane Wave Plus Local Orbitals Program for calculating Crystal Properties, University of Technology, Vienna, Austria (2008).

[39]J. Serrano, A.H. Romero, F.J. Manjon, R. Lauck, M. Cardona, A. Rubio, Phys. Rev. B 69 094306. (2004).

[30]samira chelli; Thèse de doctorat; « étude des propriétés structurales, électroniques, thermiques etthermodynamiques des alliages ternaires$BaxSr1-xS$, $BaxSr1-$, et $BaxSr1-xTe$ », université badji mokhtar-annaba (2015).

Chapter III
Results and discussions

III.1. Introduction

Recently, considerable attention has been directed toward II-VI semiconductor compounds due to their promising potential in various optoelectronic and photonic applications. Within this category, binary materials such as calcium selenide (CaSe) and zinc selenide (ZnSe) are of particular interest owing to their distinct structural and electronic properties.

To gain deeper insights into the fundamental characteristics of these materials and to provide a theoretical basis for future electronic and optical device development, we employed density functional theory (DFT) within the framework of the full-potential linearized augmented plane wave (FP-LAPW) method.

This study is focused on determining, using the WIEN2k computational package, the structural, electronic, and optical properties of the CaSe and ZnSe compounds, as well as analyzing and interpreting the results obtained from our simulations.

III.2. Calculation details

To perform our calculations, we employed the full-potential linearized augmented plane wave (FP-LAPW) method **[1]**, in accordance with density functional theory (DFT) **[2–3]**, using the WIEN2k computational package **[4]**. The aim of this work is to investigate the structural, electronic, and optical properties of the binary compounds calcium selenide (CaSe) and zinc selenide (ZnSe).

To account for the exchange-correlation interaction, we adopted the generalized gradient approximation (WC-GGA) proposed by Wu and Cohen **[5]** for the prediction of structural properties. For the electronic properties, both the WC-GGA and the modified Becke-Johnson (mBJ) potential, developed by Tran and Blaha **[6]**, were used to obtain more accurate energy band gap values. The mBJ potential was also applied for the computation of the optical characteristics of these compounds.

The FP-LAPW method is an ab initio technique designed to solve the Schrödinger equation for solid-state systems. In this method, the unit cell is divided into two regions: non-overlapping muffin-tin (MT) spheres centered on atoms, and the interstitial region between them. In the MT spheres, the basic functions, charge density, and potential are expanded in spherical harmonics up to a maximum angular momentum quantum number of l_{max}= 10. In the interstitial region, these quantities are expressed in terms of plane waves, with a cutoff defined by the product $R_{MT}K_{max} = 8$, where R_{MT} is the smallest muffin-tin radius and K_{max} is the largest wave vector in the plane-wave expansion.

For the current study, the muffin-tin radii RMT were chosen to be 2.2 a.u. for calcium (Ca), 2.3 a.u. for zinc (Zn), and 2.1 a.u. for selenium (Se). The electronic configurations considered in the calculations were as follows:

Ca [Ar] $4s^2$ **Zn [Ar] $3d^{10}$ $4s^2$**

Se [Ar] $3d^{10}$ $4s^2$ $4p^4$

III.3. Results and discussion

III.3.1. Structural properties of CaSe and ZnSe compounds

As a first step in this work, we calculated the structural properties of the binary compounds CaSe and ZnSe using the WC-GGA approximation.

In this study, we performed a self-consistent field (SCF) calculation of the total energy for different values of the lattice parameter *a*, taken near the experimental value.

These properties were determined by fitting the total energy as a function of volume using the Murnaghan equation **[7]**.

$$E(V) = E_0 + \frac{B}{B'(B'-1)}\left[V\left(\frac{V_0}{V}\right)^{B'} - V_0\right] + \frac{B}{B'}(V - V_0)$$

Where: E_0, V_0, B, and B′ represent, respectively, the total energy, the equilibrium volume, the bulk modulus (compressibility modulus), and its pressure derivative.

The bulk modulus is given by:

$$B = V\frac{\partial^2 E}{\partial V^2}$$

The figures below show the variation of the total energy as a function of volume for the binary compounds CaSe and ZnSe, using the WC-GGA approximation, for both the Zinc Blende (ZB) and Rock Salt (NaCl) phases, with the aim of investigating the stability between these two structures.

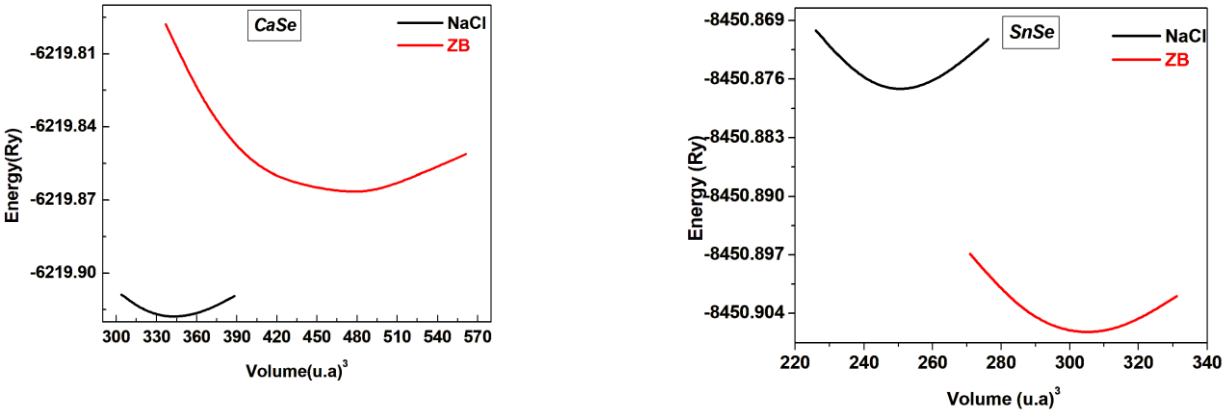

Figures III.1*.Variation of total energy as a function of volume of binary compounds CaSe and ZnSe in zinc blende and NaCl structures calculated by (WC-GGA).*

The stable phase for each compound is the one with the lowest total energy. In this case, it is clearly observed that the CaSe compound is stable in the rocksalt structure, while the ZnSe compound is stable in the Zinc Blende structure.

The numerical results obtained for the structural parameters of our binary compounds, namely the lattice parameter a and the bulk modulus B, using the WC-GGA approximation, are presented in Table (III.1).

To validate our results, the table also includes experimental and theoretical data obtained using the same method.

Lattice parameter a (A°)					**Bulk modulus B (Gpa)**			
x	**Our work (WC-GGA)**		**Exp**	**Other works (WC-GGA)**	**Our work (WC-GGA)**		**Exp**	**Other works (WC-GGA)**
	NaCl	**ZB**			**NaCl**	**ZB**		
CaSe	5.876	6.509	5.916[a]	5.829[a], 5.963[b]	52.143	34.387	51[a]	56.2[a], 47.38[b]
ZnSe	5.294	5.274	5.668[c]	5.635[c], 5.666[d]	83.224	82.626	64.7[e]	63.9[f], 67.32[d]

[a] Ref [8], [b] Ref [9], [c] Ref [10, [d] Ref [11], [e] Ref [12], [f] Ref [13].

Table III.1. *Lattice parameter a in (Å), bulk modulus B in (GPa) for the binary compounds CaSe and ZnSe compared to other experimental and theoretical data.*

The calculated lattice parameter show very good agreement with the experimental values and previous theoretical reports. For instance, the lattice constant of CaSe in the NaCl phase is

computed to be 5.876A°, which is very close to the experimental value of 5.916A°. Similarly, for ZnSe in the ZB phase, the value obtained (5.294A°) slightly underestimates the experimental value (5.668A°), a common trend observed in DFT calculations using GGA-type functional.

As for the bulk modulus B, the WC-GGA results slightly overestimate the experimental values, particularly for ZnSe in the ZB structure (82.06 GPa vs 64.7 GPa). This overestimation is also a known behavior of GGA approximations, which tend to predict stiffer materials.

Overall, the close agreement between our results and the reference data confirms the reliability and predictive power of the WG-GGA method for describing the structural properties of these II-VI semiconductors. These findings provide a solid basis for further investigations into their electronic and optical properties.

III.3.2. Electronic properties

The study of the electronic structure of compounds helps to determine their field of application, particularly for optoelectronic devices. This study mainly relies on calculating the energy band gap and its type, whether direct or indirect. The electronic properties of semiconductors stem from their electronic structures, which is why we will examine the band structure of each of our binary compounds.

Energy bands represent the possible energies of an electron. The band structure describes the relationship between an electron's energy and its wave vector $\vec{k}$ (the dispersion relation E(k)) **[14]**

III.3.2.a. Band structure and energy gap

In this section dedicated to the study of the electronic structure of binary compounds, we focused on calculating the band structures in order to determine the energy gaps of these materials.

The band structures were computed using the optimized lattice parameter obtained from our structural property calculations, specifically the one determined using the WC-GGA approximation. These band structures were calculated along the high-symmetry directions of the Brillouin zone of a cubic cell.

For the treatment of the exchange-correlation potential, as previously mentioned, the mBJ approximation was also included in our calculations alongside WC-GGA, with the aim of improving the energy gap values and bringing them closer to experimental results. This is due

to the fact that traditional DFT functionals **[2]** have consistently underestimated energy gaps compared to experimental data.

Figure (III.2) presents the band structures of the binary compounds CaSe and ZnSe calculated by the (mBJ) approximation.

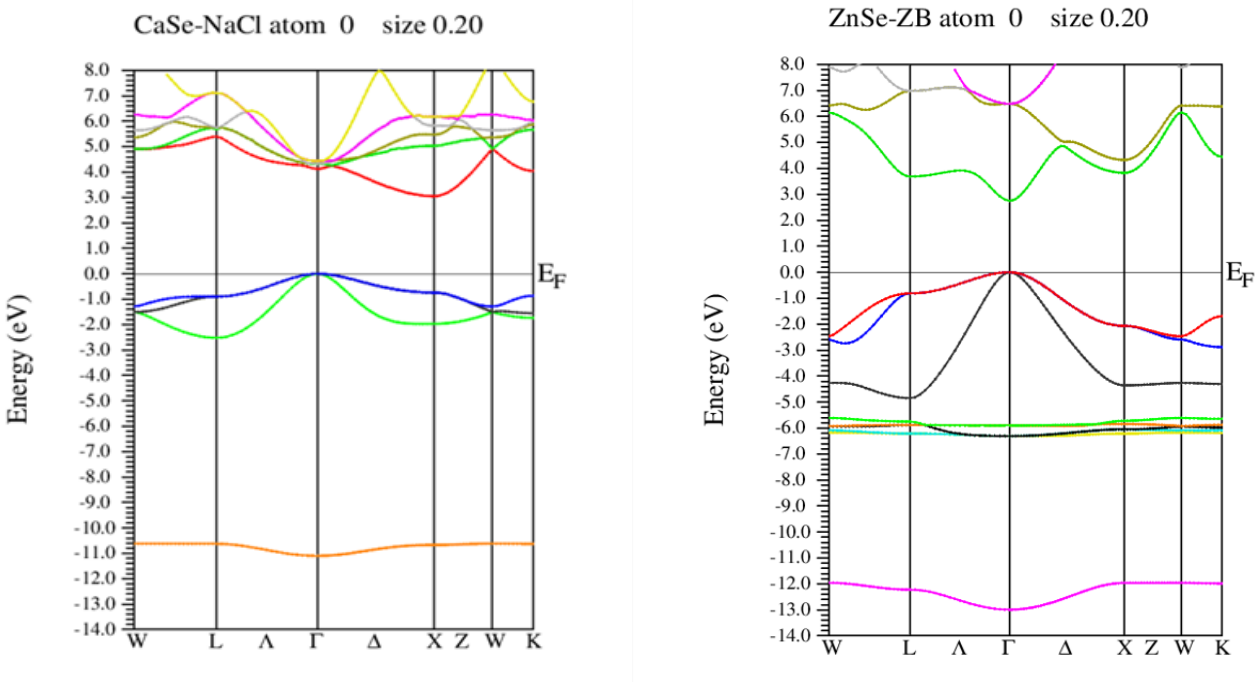

Figure III.2. *Band structure of CaSe and ZnSe compounds using mBJ approximation*

From these curves, we can observe that for the binary compound CaSe, the maximum of the valence band is located at the symmetry point Γ and the minimum of the conduction band is located at the symmetry point X. Therefore, the binary compound CaSe has an indirect band gap along the direction (Γ→X). For the compound ZnSe, the minimum of the conduction band and the maximum of the valence band are located at the symmetry point Γ. Therefore, the compound has a direct band gap along the direction (Γ→Γ).

The values of the energy gaps, calculated using the mBJ approximation, are compiled in Table (III.2). They are then compared to experimental data as well as to the results of other theoretical work.

Eg(eV)				
Composés	**Nos calculs**		**Exp**	**Autres calculs**
	WC-GGA	mBJ		
CaSe	2.14	4.12	3.85[a]	2.1[b], 2.08[b], 2.81[b]
ZnSe	1.144	2.753	2.68[c]	1.863[d], 1.848[e], 2.50[f]

[a] Ref [15], [b] Ref [16], [c] Ref [17], [d] Ref [18], [e] Ref [19], [f] Ref [20]

Table III.2. *Energy gaps of the compounds CaSe and ZnSe (in eV) with the different approximations (WC-GGA), and mBJ compared to other experimental and theoretical results*

It is evident that the mBJ method yields significantly higher band gap values than WC-GGA. This discrepancy is expected, as GGA-based approaches, including WC-GGA, are known to systematically underestimate band gaps due to their inadequate treatment of the exchange-correlation potential in semiconductors and insulators. In contrast, the mBJ potential is designed specifically to improve the description of the band structure, particularly the conduction bands, thus providing results that are closer to experimental values.

For example, in the case of CaSe, the WC-GGA predicts a band gap of 2.14 eV, while the mBJ method yields 4.12 eV, which is in better agreement with previous theoretical results (3.85 eV) and lies within the range reported in literature. Similarly, for ZnSe, the WC-GGA result (1.144 eV) is much lower than the experimental value, whereas the mBJ prediction (2.753 eV) aligns more closely with both experimental and other theoretical findings.

We can say that the mBJ method provides a more accurate estimate of the electronic band gap, making it more suitable for studying the optical and electronic properties of semiconductors such as CaSe and ZnSe.

III.3.2.b. Density of states

The density of electronic states, abbreviated DOS (Density of State), ranks among the most crucial electronic properties, providing insight into the behavior and electronic nature of a given system. Partial densities of states are derived from the total DOS, based on the atomic orbitals of each compound (s, p, d, f).

In this study, the calculation of the density of electronic states is used as a tool to validate the reliability of the band diagrams over the entire Brillouin zone, and not only in specific directions.

Figure **(**III.3) illustrates the densities of states of the CaSe and ZnSe materials by the mBJ approximation**.**

The density of state spectra of the binary compounds CaSe and ZnSe are distributed mainly in two regions:

-For the CaSe semiconductor

1-The valence band between -3 eV and the Fermi energy is mainly due to the ***p*** orbital of selenium (Se) with a slight contribution from the ***d*** orbital of calcium (Ca).

2-Above the Fermi level (conduction band), the electron density is dominated by the ***d*** orbital of calcium (Ca) and a slight contribution from the ***d*** orbital of Se.

-For the ZnSe semiconductor

1-The first region (the valence band) of the compound ZnSe, located between -6.8 eV and 0 eV, dominated mainly by the hybridization of the ***d*** orbital of Zink (Zn) and ***p*** orbital of selenium (Se).

2-In the conduction band, above the Fermi level, the electron density is dominated by the ***d*** orbital of selenium (Se).

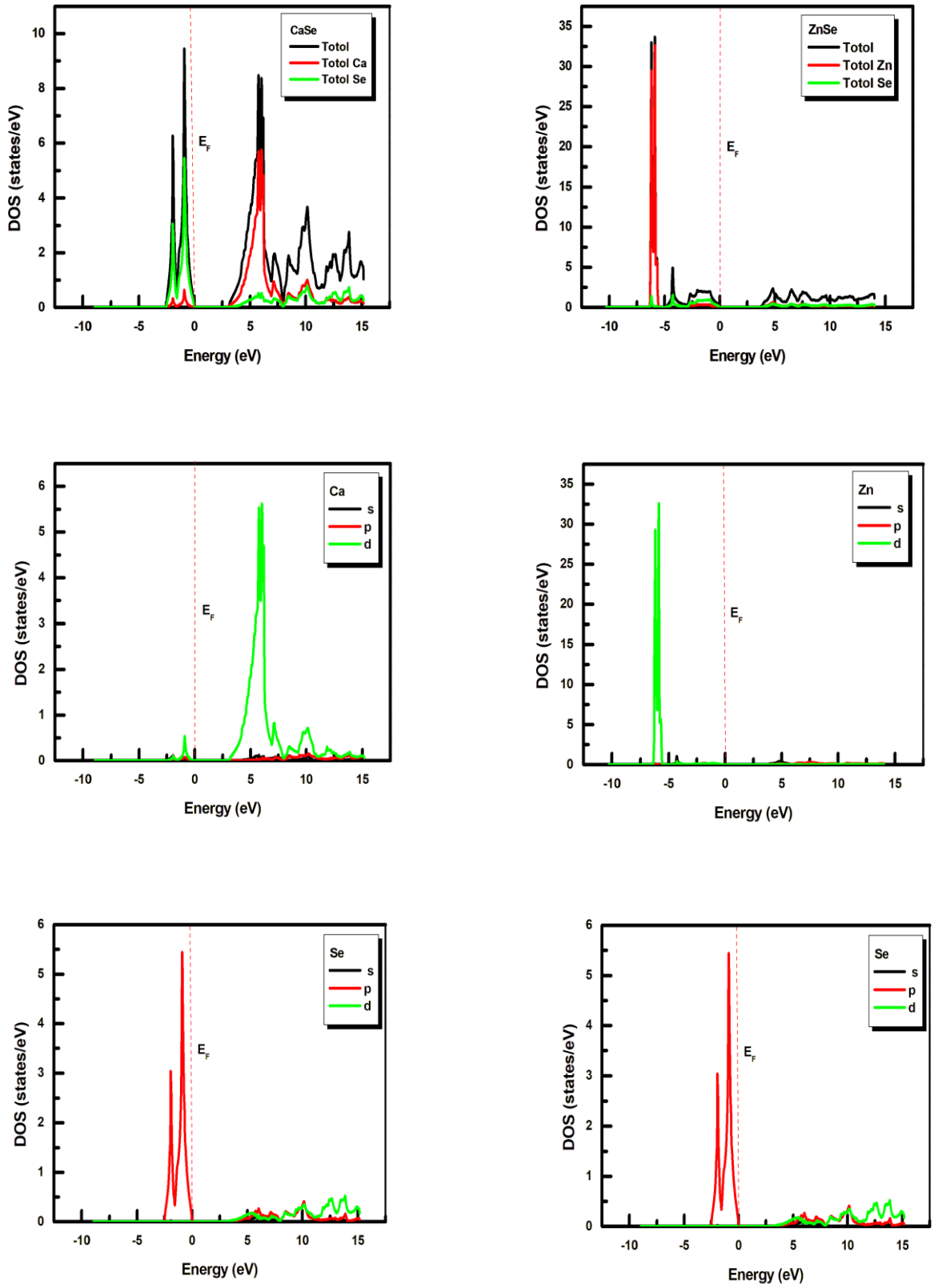

Figure III.3.*Total and partial density of states (DOS) of CaSe and ZnSe compounds using the mBJ approximation.*

III.3.3. Optical properties

Optical properties in solid-state physics result from electronic transitions between the valence band and conduction band levels. Transitions describe the interaction of electromagnetic radiation with a material and induce polarization effects. These processes constitute the material's optical response and can be characterized by the dielectric function $\varepsilon(\omega)$, which plays an important role in the study of optical properties. Determining the dielectric function $\varepsilon(\omega)$ allows us to obtain other optical quantities such as absorption, refractive index, reflectivity, and lost energy.

In this section, we focused on determining the optical properties of the binary compounds CaSe and ZnSe to understand the nature of these compounds and to provide a clear idea of their applications in optoelectronic devices.

The dielectric function $\varepsilon(\omega)$ **[21]** is the sum of two components: the real component or part $\varepsilon_1(\omega)$and the imaginary component or part $\varepsilon_2(\omega)$, such that:

$$\varepsilon(\omega) = \varepsilon_1(\omega) + i\,\varepsilon_2(\omega) \qquad \textbf{(III-3)}$$

The real part $\varepsilon_1(\omega)$ is related to the polarization, and the imaginary part $\varepsilon_2(\omega)$, depends on the electronic transition causing the absorption. Both the real and imaginary parts of the dielectric function can be obtained from the Kramers-Kronig relations **[22, 23]**:

$$\varepsilon_1(\omega) = 1 + \frac{2}{\pi} P \int_0^{\infty} \frac{\omega' \varepsilon_2(\omega')}{(\omega'^2 - \omega^2)} d\omega' \qquad \textbf{(III-4)}$$

$$\varepsilon_1(\omega) = -\frac{2\omega}{\pi} P \int_0^{\infty} \frac{\varepsilon_1(\omega') - 1}{(\omega'^2 - \omega^2)} d\omega' \qquad \textbf{(III-5)}$$

Where ω is the light frequency and P the principal value of the Cauchy integral.

Among the optical properties that describe the interaction of light with the medium is the complex refractive index $N(\omega) = n(\omega) + ik(\omega)$. These two quantities are linked by the relationship: $\varepsilon = N^2$.

It is also possible to relate the real and imaginary parts as follows:

$$\varepsilon_1(\omega) = n^2 - k^2 \qquad \textbf{(III-6)}$$

$$\varepsilon_2(\omega) = 2nk \qquad \textbf{(III-7)}$$

Knowledge of the real and imaginary parts of the dielectric function allows the calculation of optical constants. The real refractive index n(ω) and the attenuation coefficient k(ω) (extinction) are defined by the following two relations **[24, 25]**:

$$n(\omega) = \left\{ \frac{\varepsilon_1(\omega)}{2} + \frac{\sqrt{\varepsilon_1^2(\omega)+\varepsilon_2^2(\omega)}}{2} \right\}^{\frac{1}{2}} \quad \textbf{(III-8)}$$

$$k(\omega) = \left\{ \frac{\sqrt{\varepsilon_1^2(\omega)+\varepsilon_2^2(\omega)}}{2} - \frac{\varepsilon_1(\omega)}{2} \right\}^{\frac{1}{2}} \quad \textbf{(III-9)}$$

When light radiation falls on a solid body, it interacts with it by exchanging energy. The reflection coefficient characterizes the portion of energy that is reflected at the interface of this body. It is given by:

$$R(\omega) = \left| \frac{\sqrt{\varepsilon(\omega)}-1}{\sqrt{\varepsilon(\omega)}+1} \right|^2 = \frac{(n-1)^2+k^2}{(n+1)^2+k^2} \quad \textbf{(III-10)}$$

The absorption coefficient α (ω) corresponds to the energy absorbed per unit of time, volume and divided by the energy flux. It is defined by the following equation:

$$\alpha(\omega) = \frac{4\pi}{\lambda} k(\omega) \quad \textbf{(III-11)}$$

α(ω)is related to by the relation:

$$\alpha(\omega) = \frac{\varepsilon_2(\omega)}{cn} \quad \textbf{(III-12)}$$

Where c and λ: the speed of light in vacuum and wavelength respectively.

The energy lost by a fast electron passing through a material is defined by the following equation:

$$L(\omega) = \varepsilon_2(\omega)/[\varepsilon_1^2(\omega) + \varepsilon_2^2(\omega)] \quad \textbf{(III-13)}$$

At low frequency (ω = 0) and from relationship (III-8), we obtain the following relationship:

$$n(0) = \varepsilon^{1/2}(0) \quad \textbf{(III-14)}$$

In our calculations of the optical properties of the binary compounds CaSe and ZnSe using the (WC-GGA) approximation, we used the equilibrium mesh parameter and a number of 3000 points k in the Brillouin zone for our binary compounds (3 times the value of k points in the calculations of structural properties, as these calculations require high precision).

III-3-3.1. Results and discussions

a. Imaginary part of the dielectric function

The variation of the imaginary part $\varepsilon(\omega)$ of the dielectric function as a function of energy is illustrated in Figure (III-4) for our binary compounds at radiation up to 40 eV.

We can first note that the first critical points of the dielectric function, which correspond to the fundamental absorption thresholds, begin at approximately 0.12 eV and 0.21 eV for CaSe and ZnSe, respectively. These critical points originate in the optical transitions between the highest valence band and the lowest conduction band, with values corresponding to the indirect Γ→X transitions for CaSe and direct Γ→Γ for ZnSe.

The main peak, which reflects the absorption maximum, is located at 5.89 eV and 6.31 eV for the CaSe and ZnSe compounds, respectively.

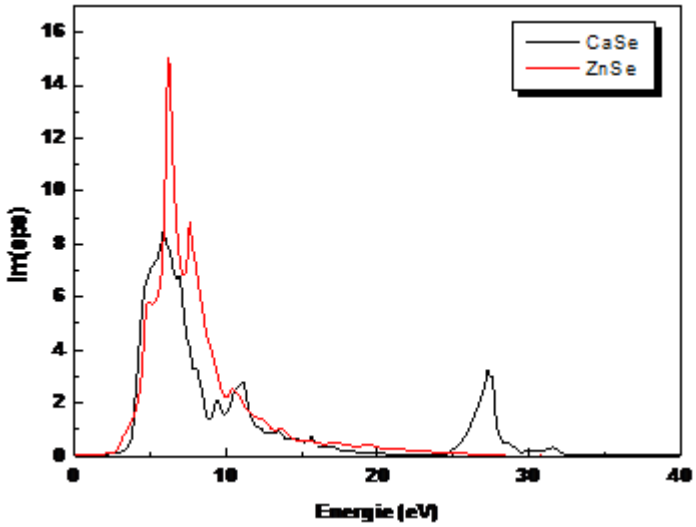

Figure III.4.*Variation of the imaginary part of the dielectric function as a function of energy for binary compounds CaSe and ZnSe*

b. Real part of the dielectric function

The real part of the dielectric function is also obtained and presented in figure (III.5) for the two binaries CaSe and ZnSe.

The zero crossing of both spectra signifies the non-existence of diffusion.

We note that for the compounds the function $\varepsilon(\omega)$ cancels at the following energy values: 6.75eV for CaSe and 6.50eV for ZnSe.

Note that at these energy values, dispersion is zero and absorption is therefore maximum.

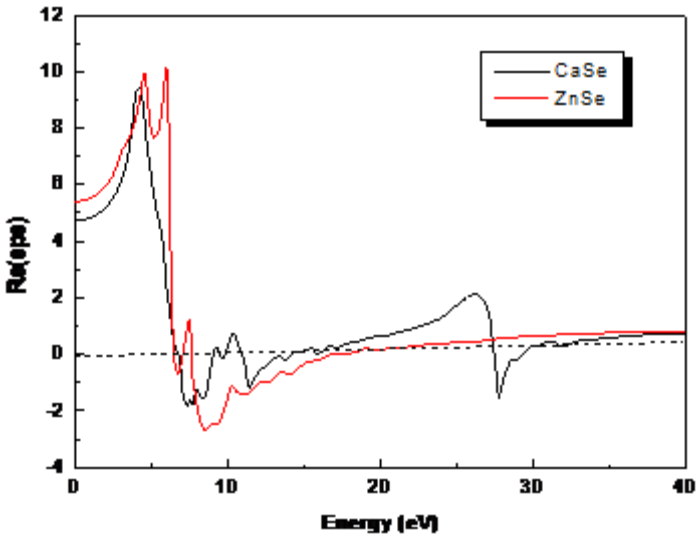

Figure III.5.*Variation of the real part of the dielectric function as a function of energy for the binary compounds CaSe and ZnSe.*

c. Refractive index

Figure (III.6) shows the variation of the refractive index as a function of energy (eV) for the binary compounds CaSe and ZnSe.

The evolution of these spectra shows that the refractive index values of the compounds CaSe and ZnSe reach a maximum value at energies 4.29 eV and 6.41 eV.

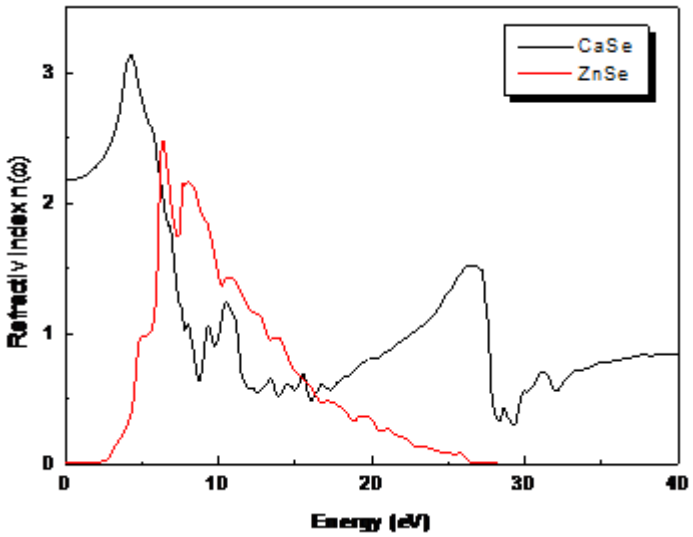

Figure III.6. *Variation of the refractive index as a function of energy for the binary compounds CaSe and ZnSe*

The static values of the refractive index n (0) and, on the other hand, the static values of the dielectric function $\boldsymbol{\varepsilon_1(0)}$ of our compounds are illustrated in Table (III.3).

Composé	Nos calculs $\varepsilon_1(0)$ WC-GGA	Autres calculs	Nos calculs $n(0)$ WC-GGA	Autres calculs
CaSe	4.75	3.22[a]	2.17	1.75[a]
ZnSe	5.44	7.50[b], 7.84[c], 6.49[d]	2.33	2.42[e], 2.54[d]

[a] Ref [26], [b] Ref [27], [c] Ref [28], [d] Ref [29], [e] Ref [30]

Table III.3. *Static dielectric function $\varepsilon_1(0)$ and static refractive index n(0) calculated for binary compounds CaSe and ZnSe.*

The calculated values of the static dielectric constant $\varepsilon 1$ (0) and the refractive index n(0) using the WC-GGA approximation for CaSe and ZnSe are found to be in reasonable agreement with previously reported results in the literature.

For both compounds, the optical constants obtained in this study fall within the expected range, although some discrepancies are observed when compared with other theoretical values. In particular, the dielectric constant and refractive index for CaSe appear slightly overestimated, while for ZnSe, the calculated refractive index shows better consistency with other available data, even though the dielectric constant is somewhat lower than values reported elsewhere.

These differences can be attributed to variations in computational methods, including the choice of exchange-correlation functional, basis sets, and convergence parameters. Such differences are common in ab initio studies and do not undermine the validity of the present results, which confirm the optical activity and semiconductor character of both materials.

d. The reflectivity spectrum

The evolution of the reflectivity of the studied binary is illustrated in Figure (III.7).

The spectra show that the reflectivity is only appreciable in a very weak ultraviolet region. As a result, the reflectivity value in the energy range [0-40 eV] is sufficient for good exploration.

The curves indicate a maximum of 48% at 27.93 eV for CaSe and 47% at 9.23 eV for ZnSe.

These results show that our binary compounds are, a priori, good candidates for use in the ultraviolet region.

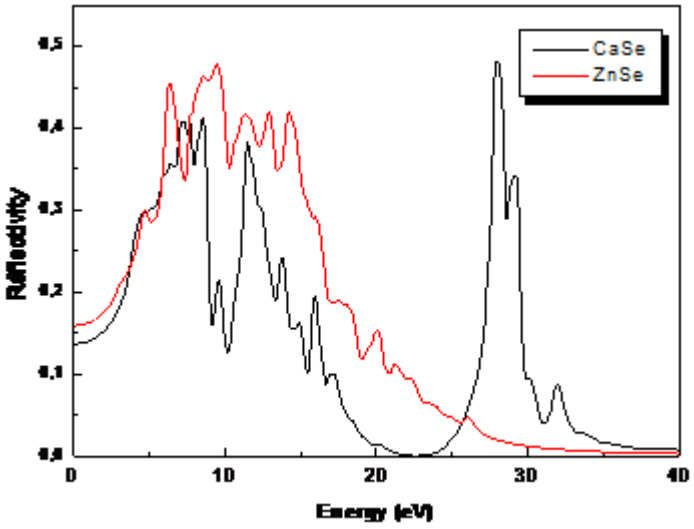

Figure III.7. *Variation of reflectivity as a function of energy for binary compounds CaSe and ZnSe*

e. Absorption

The variation of the absorption coefficient as a function of energy for our binaries is shown in Figure (III-8).

We can say that the fundamental absorption thresholds start at around 0.10 eV and 3.08 eV for CaSe and ZnSe, respectively.

The maximum energies marked on the curves equal 27.75 eV for CaSe and 8.46 eV for ZnSe.

The presence of secondary peaks around the main peak is clearly visible in these spectra.

These peaks are associated with other electronic transitions.

For example:

For secondary peaks, in the case of the CaSe compound, we have three peaks positioned around the following values 7.34 eV, 11.31 eV, 31.71 eV. And in the case of the ZnSe compound, there are two peaks around the values 6.41 eV and 11.31 eV.

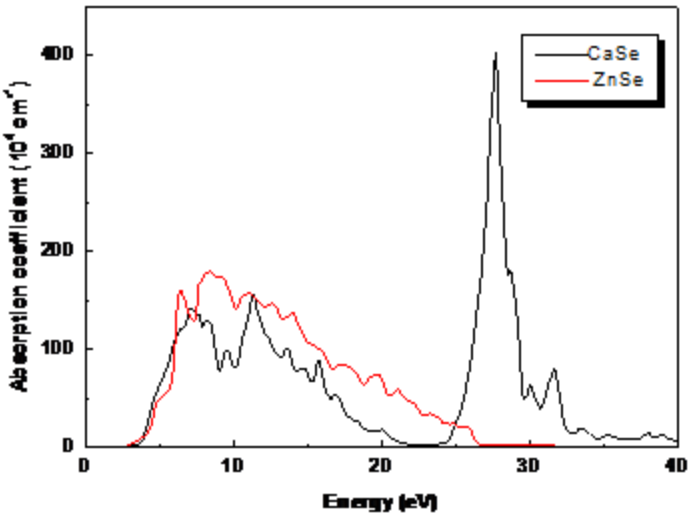

Figure III.8: *Variation of absorption coefficient as a function of energy for CaSe and ZnSe binary compounds.*

f. Electron energy loss spectrumf

The energy loss spectrum is shown in Figure (III.9).

According to this figure, the electron energy loss is maximum at 29.46 eV and 20.17 eV for CaSe and ZnSe respectively. These peaks coincide with the energies where the imaginary part of the dielectric function reaches its minimum and where the real part vanishes.

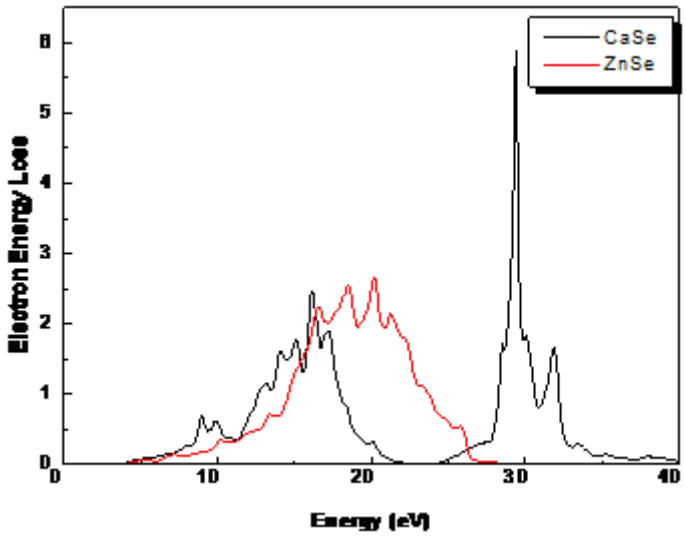

Figure III.9. *Variation of the energy loss coefficient as a function of energy for the binary compounds CaSe and ZnSe.*

References

[1] O.K. Andersen, Phys. Rev. B. 12 (8), 3060 (1975).

[2] P.Hohenberg, W. Kohn, Phys. Rev. B. 136, 864 (1964).

[3] W. Kohn, L. J. Sham, Rev. Phys. 140 (4A), A1133 (1965).

[4] P. Blaha, K. Schwartz, G .K. H.Madsen, D.Kvasnicka, J.Luittz.WIEN2K, Anaugmented plane Wave local orbitals program for calculating crystal properties, Karlheinz Schwarz, Techn. Universitat, Wien Austria, (2001).

[5] G.S. Nunes, P.B. Allen, Phys. Rev. 57; 5098(1997).

[6] F. Tran and P. Blaha, Phys Rev.Lett 102, 226401 (2009).

[7] F. D. Murnaghan,Proc .Natl .Acad.Sci.USA 30,5390 (1944).

[8] P. Cortana and P.Masri ,J.PhysCondens.Matter 10 8947-8955 (1998)

[9] S. Labidi,∗ M. Boudjendlia, M. Labidi, and R. Bensalem Department of Physics, Faculty of Sciences, BadjiMokhtar University, P.O. Box 12, 23000 Annaba, Algeria (Received March 1, 2013)

[10] H. Okuyama, Y. Kishita, and A. Ishibashi, Phys. Rev. B 57, (1998) 2257

[11] R. Gangadharan, V. Jayalakshmi, J. Kalaiselvi, S. Mohan, R. Murugan, B. Palanivel, J. Alloy. Compd. 5 (2003) 22

[12] B.H. Lee, J. Appl. Phys. 41 (1970) 2988

[13] S.-G. Lee and K. J. Chang, Phys.(1995) Rev. B 52, 1918

[14] Bendaif Samira; thèse de doctorat; «Etude des propriétés structurales, électroniques, thermodynamiques et thermiques des alliages quaternaires Zn1-XCdXSySe1-y», université Badji Mokhtar–Annaba (2015)

[15] Y. Kaneko and T.Koda. J. Cryst. Growth 86, 72 (1988).

[16] Z. Charifi ,H. Baaziz ,F. ELHaj Hassan ,N. Bouarissa,J. Phys : Condens .Matter.17,4.83(2005).

[17] O. Madelung (ed.), Londolt-Börnstein New Series III, Springer, Berlin, (1987), Vol. 22.

[18] El Haj Hassan F, Amrani B and Bahsoun F (2007) Physica B 391-365.

[19] K. Hacini, H. Meradji, S. Ghemid and F. El Haj Hassan (2012) Chin. Phys. B Vol. 21, No. 3. 036102.

[20] A. M. Saitta, S. de Gironcoli, and S. Baroni, Appl. Phys. Lett. 75, 2746 (1999).

[21] O. Madelung (Ed.), Numerical Data and Functional Relationship in Science and Technology, Landolt Bo rnstein, New Series Group III, vol. 17, Springer-Verlag, Berlin, (1982).

[22] C. A. Draxl, R. Abt, ICTP lecture notes, unpublished, (1998).

[23] **[**P. Y. Yu, M. Cardona, Fundamentals of Semiconductors, Physics and Materials Properties. Berlin: Springer-Verlag, 233 (1999).

[24] F. Koostra, P.L.deBoeij, J.G Snijders, Phys. Rev. B 62, 7071 (2000).

[25] W.Y. Ching, F. Gan and M.Z. Huang, Phys. Rev. B 52, 1596 (1995).

[26] Ahmad, I., Alam, Q., Ahmad, A., & Muhammad, S. (n.d.). Theoretical aspects of structure, electronic, optical and elastic properties of Ca(1−x)CxSe mixed alloys in binary and ternary phases. Department of Physics, Hazara University; School of Physics, University of Electronic Science and Technology of China

[27] Ali Hussain Reshak, Sushil Auluck, Phys. B 388 (2007) 34.

[28] You Yu, Jingjing Zhou, Huilei Han, Chuanyu Zhang, Tuo Cai, Chengqun Song, Tao Gao. Journal of Alloys and Compounds 471 (2009) 492–497.

[29] G. Surucu, K. Colakoglu, E. Deligoz, N. Korozlu, Y.O. Ciftci. Solid State Communications 150 (2010) 1413-1418.

[30] M. Rabah, B. Abbar, Y. Al-Douri, B. Bouhafs, B. Sahraoui. Materials Science and Engineering B100 (2003) 163-171.

Conclusion Générale

General conclusion

We studied the structural, electronic, and optical properties of the binary compounds CaSe and ZnSe using the linearly augmented plane wave (FP-LAPW) method within the framework of density functional theory (DFT), implemented in the Wien2K code. Our results are presented as follows:

The study of structural properties allows us to predict the most stable phase of the materials. We presented the variation of total energy as a function of volume for the compounds CaSe and ZnSe, calculated using the WC-GGA approximation in both NaCl and ZB structures. We found that the CaSe compound is stable in the rocksalt structure (NaCl), while the ZnSe compound is stable in the Zinc Blende structure (ZB).

In the next step, we calculated the equilibrium quantities for our binary compounds, namely the lattice parameter **a** and the bulk modulus **B** in the two phases studied. These quantities agree well with the theoretical values available in the literature, and are also close to the experimental results.

Next, we studied the electronic properties in the most stable phase and noted that: The results obtained from the energy band gaps of our binary compounds, calculated using the WC-GGA and mBJ approximations, show good agreement with previous theoretical studies. The binary compound CaSe is found to be an indirect band gap semiconductor, with the transition occurring along the Γ→X direction. In contrast, for the compound ZnSe, both the minimum of the conduction band and the maximum of the valence band are located at the Γ point, indicating that it is a direct band gap semiconductor along the Γ→Γ direction. We studied the total and partial densities of states (DOS) of each binary compound.

Finally, optical properties such as the dielectric function ε(ω) as well as the refractive index, the absorption coefficient, the reflectivity and the lost energy were also calculated. This study shows that the binary compounds CaSe and ZnSe are a priori good candidates for use in the ultraviolet range.